Reducing hepatocyte injury and necrosis in response to paracetamol using non-coding RNAs

Reducing hepatocyte injury and necrosis in response to paracetamol using non-coding RNAs

Dagmara Szkolnicka[1], Baltasar Lucendo-Villarin[1], Joanna K. Moore[1], Kenneth J. Simpson[2], Stuart J. Forbes[1], David C. Hay[1*]

1. Medical Research Council Centre for Regenerative Medicine, University of Edinburgh, Edinburgh, United Kingdom.
2. Division of Clinical and Surgical Sciences, University of Edinburgh, Edinburgh, United Kingdom

*** Corresponding Author**:

Dr David C. Hay, PhD, MRC Centre for Regenerative Medicine, University of Edinburgh, 5 Little France Drive, Edinburgh EH16 4UU, Scotland, United Kingdom. davehay@talktalk.net, Telephone: +441316519549, Fax: +441316519501

Financial support:

We thank Sistemic (www.sistemic.co.uk; Glasgow) for performing the microRNA profiling experiments. The microRNA profiling experiments were funded by the Scottish Stem Cell Network. Ms Dagmara Szkolnicka and Mr Baltasar Lucendo Villarin were supported by MRC PhD Studentships. Drs Hay and Forbes were supported by awards from the UK Regenerative Medicine Platform (MR/K026666/1 and MR/L022974/1). Dr Simpson received support from the Chief Scientist Office, Scotland (ETM/191).

Conflict of interest:

The authors have no conflict of interest to declare

Author's contributions:

Dagmara Szkolnicka: Conception and design; collection and/or assembly of data, data analysis and interpretation; manuscript writing and proof-reading.

Baltasar Lucendo-Villarin: collection and/or assembly of data, data analysis and interpretation

Kenneth Simpson: provision of patient samples, data analysis and interpretation, manuscript proof reading.

Joanna Moore: provision of patient samples, data analysis and interpretation.

Stuart J Forbes: supervision, data analysis and interpretation, manuscript proof reading.

David C. Hay: Conception and design, supervision, data analysis and interpretation, manuscript writing; financial support, final approval of manuscript and proof-reading.

Key words:

Drug induced liver injury; micro RNA, hepatocyte, apoptosis, necrosis, paracetamol.

ABSTRACT

The liver performs multiple functions within the human body. The liver is composed of numerous cell types which play important roles in organ physiology. Our study centres on the major metabolic cell type of the liver, the hepatocyte, and its susceptibility to damage during drug overdose. In these studies hepatocytes were generated from a renewable and genetically defined stem cell resource. In vitro derived hepatocytes were extensively profiled and exposed to varying levels of paracetamol and plasma isolated from liver failure patients, with a view to identifying non-coding micro-RNAs which could reduce drug or serum induced hepatotoxicity. We identified a novel anti-microRNA which reduced paracetamol induced hepatotoxicity and glutathione depletion. Additionally, we also demonstrated a **pro-survival** role for anti-microRNA-324 in response to plasma collected from liver failure patients. We believe that these studies represent an important advance for the field, demonstrating the power of stem cell derived systems to model human biology 'in a dish' and identify novel non-coding microRNAs which could be translated to the clinic in the future.

INTRODUCTION

The liver is a multi-functional and highly regenerative organ. In both the acute and chronic settings liver disease has dire consequences for health. A common cause of liver damage is adverse reactions to drugs which can lead to drug induced liver injury (DILI). This creates major problems for patients, clinicians, the pharmaceutical industry and regulatory authorities (Olsen and Whalen, 2009). It has been reported that in the United Kingdom (UK) approximately 15% of the hospital in-patients suffer from liver toxicity in response to medicines during admissions, with 20% of these patients readmitted again after one year and a 2% mortality rate (Davies *et al*, 2009, Davies *et al*, 2010;). The annual cost to the National Health Service in the UK ~£450 million with the costs growing year by year (Pirmohamed, 2004).

In the context of drug overdose or serious adverse reactions, liver failure can be acute and life threatening, and in some cases require orthotopic liver transplantation. While transplantation is highly successful, such an approach has many limitations (Szkolnicka *et al* 2014a) and justifies basic science attempts to develop better human models to study liver injury and cost effective and scalable intervention strategies. With this in mind, we have studied the importance of microRNAs (miRs) in regulating human drug metabolism and their potential to reduce liver toxicity in response to toxic levels of paracetamol.

miRs are small non-coding RNAs that are approximately 20 - 24 nucleotides long and their major function is to fine tune gene expression of target their genes. Enzyme processing of primary and precursor microRNAs generates a mature microRNA that is incorporated to the RNA-induced silencing complex (RISC). The complex recognizes the target mRNA through perfect and imperfect base pairing with the target miRs (Bartel, 2009). Recently, it has been demonstrated that microRNAs play a role in regulating the first phase of drug metabolism (Pan *et al*, 2009a; Tsuchiya *et al*, 2006; Yu, 2009; Yu and Pan, 2012) as well as play an

essential role in controlling phase III transporters important in drug efflux (Kovalchuk *et al*, 2008; Zhu *et al*, 2008). However the second phase of drug metabolism, drug conjugation, has not been studied in detail. Drug conjugation is crucial in human drug metabolism, and any alternations in this process can lead to massive hepatocyte death and acute liver failure, which can be life threatening. To test the importance of miRs in regulating phase II drug metabolism we opted to study the metabolism of a **commonly** used analgesic, paracetamol. When taken in the appropriate amounts paracetamol is modified by sulfuryl transferases and UDP glucuronosyl transferases and removed from the body without organ damage (Chun *et al*, 2009). However, when paracetamol is taken above the recommended dose it is metabolised by phase I enzymes to generate a toxic intermediate N-acetyl-p-benzoquinone imine (NAPQI), which if untreated can lead to hepatocyte cell death and liver failure, placing the patient in a life threatening situation. In order to promote non-toxic drug metabolism, in the context of drug overdose, we identified and employed candidate miRs to regulate the different steps of paracetamol metabolism.

In summary, we have identified a novel microRNA which regulates phase II drug metabolism promoting non-toxic paracetamol drug metabolism, thereby reducing hepatic cytotoxicity. Moreover, we demonstrate a supportive role for microRNAs in managing the toxic nature of human liver failure plasma. We believe our findings are novel and provide proof of concept. These studies exemplify the power of pluripotent stem cell derived models ‘in a dish’ to identify new approaches to treating human liver damage.

METHODS AND MATERIALS

Cell Culture and Differentiation

hESCs (H9) were cultured as described in (Hay *et al*, 2008; Hay *et al*, 2011) and maintained in a humidified 37 °C, 5% CO_2 incubator. The cells were differentiated as described previously (Szkolnicka *et al*, 2014a; Szkolnicka *et al*, 2014b).

Primary Human Hepatocyte Culture

The cryopreserved human primary hepatocytes were purchased from Life Technologies. In this study, female line (Hu8119; HMCPIS) and male line (Hu8182; HMCPIS) were chosen. Both lines were donated from Caucasian patients of 21-27 years of age. The cryoplateable hepatocytes were plated and maintained as per vendor's instruction. Briefly, hepatocytes were resuspended in thawing medium (CM3000) and plated onto matrigel in a 48-well plates. Subsequently, cells were placed in the incubator at 37°C (5% CO_2) for 24 hours. At 24 hours post-replating, the medium was changed to incubation medium (CM4000). At 48 hours post-replating, hepatocyte metabolic activity (CYP3A and CYP1A2) were measured using Promega luciferase-based assay.

RNA Isolation and Quantitative Polymerase Chain Reaction for SULT2A1 and GSTT1

The RNA was isolated, reversely transcribed and used for TaqMan polymerase chain reaction as described in Szkolnicka *et al* (2014a). The reference numbers of particular primers can be found in Supplementary Table 4.

RT² Profiler PCR Array

The total RNA of hESC-derived hepatocytes (day 18) and Primary Human Hepatocytes (purchased from 3H Biomedical AB, Sweden) was reverse transcribed using RT² First Strand Kit (QIAGEN) as per manufacturer's instructions. The qPCR reaction was set up using RT² Profiler PCR Array (Human Drug Metabolism Array, Human Drug Metabolism Phase II Enzymes Array, and Human Drug Transporters Array were purchased from QIAGEN) as per manufacturer's instructions.

MicroRNA Profiling

The total RNA of hES-derived hepatocytes (day 18; n=3) and Primary Human Hepatocytes (purchased from 3H Biomedical AB) were analysed on Agilent miRNA platform (using Agilent's SurePrint G3 Human v16 microRNA 8x60K microarray slides; miRBase version 16.0) following Sistemic **proprietary SOPs**. One 100 ng of total RNA, from a working solution at 50ng / ul in nuclease-free water, was used as input for each microarray experiment. Each slide contained 8 individual arrays, each array was identified by a unique barcode and contained capture probes for 1349 microRNAs (1205 Human; 144 viral). The microarray data were normalized using Sistemic's in-house pre-processing and data quality control (QC) methods. Detection calls (present or absent) for individual miRNAs were compared across the samples. The detection calls were calculated using the Agilent Feature Extraction (AFE) software version 10.7.3.1. A detailed description of how these calls are made is available in the Feature Extraction Reference Guide on the Agilent website (http://www.genomics.agilent.com)

MiR – mRNA Binding Analysis

TargetScanHuman6.2 is an online tool that predicts microRNA binding sites at the 3'UTR of the biological target. The programme focuses on the presence of conserved and non-conserved sites that match the seed region of each microRNA (Lewis *et al*, 2005).

Immunofluorescence

Cell cultures at day 18 of cellular differentiation were fixed in 100% ice-cold methanol at -20°C for 30 minutes. After fixation, cell cultures were washed twice with PBS at room temperature. Cells were blocked with 0.1% PBS-Tween containing 10% BSA for 1 hour and subsequently incubated with primary antibodies diluted in PBS-0.1% Tween/1% BSA (the GSTT1 antibody was diluted in PBS-0.1% Tween/2% BSA) at 4°C overnight. The following day, the primary antibody was removed, and the fixed monolayers were washed three times with PBS-0.1% Tween/1% BSA (the GSTT1 antibody was washed in PBS-0.1% Tween/2% BSA). Following this, the cells were incubated with the appropriate secondary antibody diluted in PBS for 1 hour at room temperature and washed three times with PBS. After washing, the Hoechst 33342 (NucBlue® Live Cell Stain Ready Probes; Life Technologies) diluted in PBS (as per manufacturer's instructions) was added to the culture and incubated for 20 minutes at room temperature. Subsequently, the solution was removed and cell cultures were mounted with Mountant PermaFluor (Thermo Scientific). The cells were analyzed by Olympus TH4-200 microscope and Volocity 4 software. The percentage of positive cells and standard deviation were estimated from at least four random fields of view and quoted as ± standard error. The list of antibodies and dilutions are provided in Supplementary Table 4.

Paracetamol – Induced Toxicity (Toxicity Testing)

Paracetamol (Sigma- Aldrich) was diluted in ethanol (Sigma-Aldrich) and prepared at 0.5 M stock concentration. Different paracetamol concentrations (0 mM, 1 mM, 2 mM, 5 mM, 10 mM, 20mM, and 50 mM) were prepared by diluting the stock solution in specific volumes of HepatoZYME™ supplemented with factors (10 ng/ml HGF; 20 ng/ml OSM) and 2% Bovine Serum Albumin (Sigma- Aldrich). At day 17, cells were treated with specific drug concentration and left for 24 hours in the incubator at 37°C. At day 18 ATP production was measured by the CellTiter®-Glo (Promega). For primary human hepatocytes, the cells were treated with the same range of paracetamol concentrations as above at 48 hours post-replating. The concentrations were prepared by diluting the stock solution in specific volumes of incubation medium (CM4000) and 2% Bovine Serum Albumin (Sigma – Aldrich). Cells were incubated with the drug for 24 hours at 37°C. Subsequently, ATP production was measured by the CellTiter®-Glo (Promega).

In Vitro Modulation of Paracetamol Toxicity by MicroRNAs

At day 17, cells were transfected with scrambled controls or antagomirs to miR-24, miR-324 for 24 hours at 37 °C. Once transfected, hESC-derived hepatocytes were exposed to the concentration of paracetamol resulting in 50% death (IC50) for another 24 hours. At day 19, the toxic effect of the drug was measured using CellTiter – Glo® Luminescent Cell Viability Assay (Promega) and GSH/GSSG-Glo™ Assay (Promega).

In Vitro Modulation of Paracetamol Toxicity by N-acetylcysteine (*NAC)*

N-acetylcysteine (NAC; Sigma –Aldrich) was diluted in sterile water and prepared at 1M concentration. At day 17, hESC-derived hepatocytes were treated with 1mM NAC (optimal concentration determined from a range of 0-1.25mM) diluted in specific volumes of HepatoZYME™ supplemented with factors (10ng/ml HGF; 20 ng/ml OSM). At day 17, cells were treated with specific drug concentration and left for 24 hours in the incubator at 37°C. At day 18 the paracetamol toxicity was measured by the CellTiter®-Glo Luminescent Cell Viability Assay from Promega.

Cell Viability Assay

Cellular ATP levels were measured using CellTiter – Glo® Luminescent Cell Viability Assay (Promega) as per manufacturer's instructions and the luminescence signal was detected by the luminometer (Promega; Madison, WI, http://www.promega.com). The IC50 (the concentration of the compound resulting in 50% death) of paracetamol (APAP) was estimated from the function $f(x) = ax + b$.

Reduced Glutathione Depletion Assay

The amount of reduced glutathione produced in the hESC-derived hepatocytes was measured by GSH/GSSG-Glo™ Assay from Promega (Madison, WI) and carried out as per the manufacturer's instructions (http://http://www.promega.com/tbs/tb325/tb325.pdf).

Patient Information, Sample Collection, Processing

Ethical approval for the study was from the Scotland 'A' Research and Ethics Committee and written informed consent was obtained. Three female donors or their nominated next of kin consented to blood sampling. Paracetamol hepatotoxicity was prospectively defined as previously described (Craig *et al,* 2013). Peripheral blood samples were obtained on the day of admission to the Scottish Liver Transplantation Unit. Serum was collected after **centrifuging** of blood samples at 1000 *g* for 15 minutes and 4 ^{o}C within 1 hour following collection, immediately aliquoted and stored and -80 ^{o}C until thawing for the experiments. Importantly, no paracetamol was detectable in the serum samples used in the study. Patient blood biochemistry and normal ranges are provided in Supplementary Table 5.

Supplemental Information

Supplemental information includes 5 figures and 5 tables.

RESULTS

Defining Metabolic Gene Expression in Stem Cell Derived Hepatocytes.

hESC-derived hepatocytes were produced *in vitro* using established methodology (Szkolnicka *et al,* 2014a, Szkolnicka *et al*, 2014b) and demonstrated appropriate cell morphology, expression of liver transcripts and displayed appreciable levels of metabolic function (Figure 1 A-C). Cyp3A activity in stem cell derived hepatocytes was estimated at 8.4% of the female and 22% of male adult hepatocytes (Figure 1C; Supplementary Figure 1). Whereas, Cyp1A2 activity was estimated to be 0.009% and 0.06% of female and male hepatocytes respectively (Figure 1C; Supplementary Figure 1). Post validation, stem cell derived hepatocytes were characterised for drug metabolising gene expression using microarray technology. Throughout these studies, stem cell derived hepatocytes were compared to freshly isolated primary human hepatocytes. From these studies we demonstrated that stem cell derived hepatocytes expressed transcripts for phase I, II and III drug metabolism, albeit at reduced levels in comparison to primary hepatocytes (Figure 2; Supplementary Table 1).

Detailed Study of Paracetamol Metabolism in Stem Cell Derived Hepatocytes.

In order to ascertain which metabolic pathways were intact, the data from the array experiments **were** analysed using Pharma KGB software (www.pharmgkb.org). From the analysis we determined that a number of metabolic pathways were intact in our stem cell derived system, including paracetamol metabolism (Supplementary Figure 2). When paracetamol is taken within the therapeutic range **it** is metabolised and excreted normally by phase II and III enzymes (Supplementary Figure 2). However, if the drug is taken at higher doses than recommended, phase I enzymes generate N-acetyl-p-benzoquinone imine

(NAPQI) which is toxic and leads to glutathione depletion and ultimately cell death (Supplementary Figure 2). The results generated from the array experiments were validated by immunostaining, focussing on key phase II and phase III proteins. Phase II enzymes from the non-toxic pathway, SULT2A1, and toxic pathway, GSTT1, were expressed in 59% and ~98% cells respectively (Figure 3A; Supplementary Table 1). Importantly, stem cell derived hepatocytes also expressed phase III drug transporters important in each pathway. Approximately 52% and 77% of cells expressed ABCG2 and ABCC1 respectively (Figure 3A; Supplementary Table 1). We therefore hypothesised that stem cell derived hepatocytes possessed the correct machinery to process paracetamol in a non-toxic and toxic manner (Figure 3B). To test this we exposed stem cell derived hepatocytes to a range of concentrations of paracetamol, ranging from 0 to 50 mM. Following exposure, cell viability was monitored by ATP production. From these studies we demonstrated that stem cell derived hepatocyte cell death increased in a dose dependent fashion with an IC50 value of 12.85 mM. Although differences in cytochrome P450 metabolic capacity were identified between stem cell derived hepatocytes and primary hepatocytes, the paracetamol IC50 values obtained in vitro were comparable to both female and male hepatocytes, **10.51 mM and 12.6 mM respectively** (Supplementary Figure 3).

Identification of Novel MicroRNAs Within Stem Cell Derived Hepatocytes

Once we had established that stem cell derived hepatocytes responded to paracetamol appropriately, we wished to study microRNA (miR) expression within stem cell derived hepatocytes. miRs are known to be potent regulators of gene expression, and our hypothesis was that miRs could play an important role in modulating paracetamol metabolism and therefore drug overdose **in hepatocytes**. To screen for miRs which regulate this process, day 18 hESC-derived hepatocytes were harvested and analysed using Agilent miRNA platform.

From these studies we determined that stem cell derived hepatocytes and primary human hepatocytes expressed 367 miRs in common, with 220 miRs being expressed at similar levels and 147 miRs differentially expressed (Figure 4A and B; Supplementary Table 2). Of note, the major miR expressed in the liver, miR-122, was expressed at similar levels between primary and hESC derived hepatocytes (Figure 4C). Next, we evaluated similarly expressed miRs using TargetScanHuman6.2 (www.targetscan.org) to predict novel miRs which may regulate phase II enzymes important in paracetamol metabolism. The 'hits' from our screen were ranked based on the predicted efficacy using the context + scores (Friedman *et al*, 2009 and Grimson *et al*, 2007). Our analysis predicted that miR 24 and 324 could potentially regulate GSTT1 and SULT2A1 respectively, and those miRs served as the focus of further experimentation (Supplementary Table 3).

MicroRNA 324 Regulates Paracetamol Induced Toxicity in Stem Cell Derived Hepatocytes

In order to test our hypothesis that stem cell derived hepatocyte susceptibility to paracetamol overdose could be regulated by miRs, we transfected synthetic inhibitory non-coding RNAs. Stem cell derived hepatocyte transfection was optimised and miRs and antagomirs were used at a concentration of 50 nM for 24 hours prior to incubation with a toxic dose of paracetamol. In order to examine the effects of antagomir transfection on phase II enzyme expression, we performed qPCR and immunostaining. hESC-derived hepatocytes transfected with the scrambled control served as our baseline throughout. In response to transfection with the antagomir for miR 324, stem cell derived hepatocytes expressed greater SULT2A1 gene and protein expression. (Figure 5A and B). In contrast, transfection with miR-324 or the non-coding RNAs for miR-24 did not result in gene expression changes, nor dramatic alterations in cell viability and reduced glutathione levels (Supplementary Figures 4 and 5). Once we had established that SULT2A1 expression could be modulated successfully, we measured cell

viability in response to a 50% toxic dose of paracetamol for 24 hours, by measuring ATP depletion (IC50). The fold increase in cell viability was comparable with the cell viability enhanced by **N-acetylcysteine** (NAC) (Figure 5C). Notably increased cell viability was paralleled by a two fold increase in reduced glutathione levels (Figure 5D).

MicroRNA 324 Reduces Cell Necrosis in Response to Plasma from a Patient With Fulminant Hepatic Failure.

Following on from acute paracetamol induced hepatocyte injury, we studied the toxic nature of patient**'s** derived plasma on stem cell derived hepatocytes. As before stem cell derived hepatocytes were differentiated and transfected with either the scrambled control or the antagomir for miR-324. Twenty four hours post transfection, stem cell derived hepatocytes were incubated with human plasma from three female donors (anonymised patient details and blood biochemistry is supplied in Supplementary Table 5). Following exposure to plasma, stem cell derived hepatocyte ATP levels were measured. Notably, stem cell derived hepatocytes transfected with antagomir 324 displayed greater levels of ATP which was significantly increased over scrambled controls in two out of three patients (Figure 6A). In line with ATP, we also measured caspase 3 and 7 activity in stem cell derived hepatocytes. As for ATP, we also observed a significant increase in caspase activity following transfection with antagomir 324 in two out of three patients (Figure 6B). Taken together these data suggest that increasing the levels of SULT2A1 gene expression redirected cell necrosis to apoptosis, following challenge with plasma from patient with fulminant hepatic failure.

DISCUSSION

Despite major progress in the knowledge and management of human liver injury, there are approximately 2000 cases per year of acute liver failure (ALF) in the United States (Hoofnagle, 1995; Polson *et al* 2005; Fontana, 2008). Paracetamol overdose is a major **cause of** ALF, with critical damage done to the hepatocyte compartment of the liver, and accounts for approximately 50% of cases (Nourjah *et al*, 2006; Bari and Fontana, 2014). Although hepatocyte cell death occurs in large numbers, the manner by which the cells die following overdose remains complicated and controversial (Jaeschke *et al* 2012).

The hepatotoxic dose of paracetamol is considered to be greater than 75mg/kg. This translates into toxic blood concentrations that range between 25-150 mg/l (Winek, 1994 and Dollery, 1993). Currently, treatment with N-acetylcysteine (NAC) is the most effective strategy in treating paracetamol-induced liver injury. Patients that have ingested 75-150 mg/kg/24h can be considered for NAC treatment, with NAC usually prescribed if > 150mg/kg was ingested within 24 hours (based on the guidelines issued by the National Poisons Information Service UK; www.npis.com). Although successful, oral and intravenous NAC treatment may elicit serious side effects (Harrison *et al*, 1990; Bailey and McGuigan, 1998; Appleboam *et al*, 2002; Pakravan *et al*, 2008) and therefore new approaches to treat acute intoxication are necessary. In order to study the important nature of microRNAs in human drug toxicity, reliable and renewable liver models are required. In this vein, we have employed pluripotent stem cells to generate human hepatocyte like cells. The in vitro model employed in these studies **is** serum free and has already which has demonstrated promise in modelling human drug metabolism and toxicity testing (Szkolnicka *et al*, 2014a; Szkolnicka *et al*, 2014b; Medine *et al*, 2013; Zhou *et al*, 2014, Cameron, *et al* 2015). Moreover, in these studies we

support those observations as stem cell derived hepatocytes display similar IC50 values to male and female primary hepatocytes (Supplementary Figure 3).

MicroRNAs are potent non-coding RNAs which can alter mammalian gene expression and therefore represent promising candidates for modulating enzymatic pathways (Pan *et al*, 2009a; Tsuchiya *et al*, 2006; Yu, 2009; Yu *et al*, 2010; Yu and Pan, 2012; Kovalchuk *et al*, 2008; Zhu *et al*, 2008) and treating human disease. Several studies have shown that regulation of different microRNAs may potentially serve as effective therapeutics (Thong *et al*, 2014; Heidet and Gubler, 2009, Daige *et al*, 2014). In the recent years there has been a focus on miR regulation of phase I enzymes involved in human drug metabolism. Studies have demonstrated that miR-27b regulates CYP3A4 and CYP1B1 and miR-126* controls CYP2A3 expression (Pan *et al*, 2009a; Tsuchiya *et al*, 2006; Kalscheuer *et al*, 2008). Other studies have also focused on microRNA regulation of drug transporters such as P-glycoprotein and breast cancer resistant protein (Kovalchuk *et al*, 2008; Zhu *et al*, 2008; Liao *et al*, 2008; To *et al,* 2008, Pan *et al*, 2009b). While phase I and phase III of drug metabolism have been studied, there is still little known about regulation of phase II enzymes by microRNAs. Phase II enzymes, such as glutathione-s-transferases (GSTs) and sulfotransferases (SULTs), are essential to sufficiently detoxify different xenobiotics, therefore these enzymes serve as important clinical targets. In order to test whether microRNAs could potentially regulate phase II enzymes (SULT2A1 and GSTT1) that play an important role in paracetamol metabolism, we used TargetScan Human software to determine precise miR-gene binding interactions and used lipofectamine-based transfection to examine their supportive effects. Inhibition of miR-324-5p in hESC-derived hepatocytes resulted in increased SULT2A1 expression (Figure 5A and 5B). This led to improved cell survival in vitro, in a matter comparable with current clinical practice, NAC administration (Figure 5C).

Notably, the inhibition of miR-324-5p was paralleled by an increase in reduced glutathione production (Figure 5D). In contrast, inhibition of miR-24-3p did not have any effect on GSTT1 expression, cell viability and reduced glutathione production in the paracetamol studies. Although TargetScan has been widely used, and is considered to be the most effective in predicting miR-target binding sites (Baek *et al,* 2008; Witkos *et al*, 2011), algorithm prone errors may have led to this false prediction.

Given the promising effects of the antagomir 324 delivery in response to paracetamol, we were keen to assess its efficacy after exposure to liver failure serum from paracetamol poisoned female patients. Importantly, paracetamol was not present in patient sera and therefore we were studying the supportive effects of antagomir 324 in the context **of** patient recovery. The inhibition of miR-324-5p, by antagomir 324, resulted increased cell viability and caspase activity in 2 patients (Figure 6) suggesting a potential switch from cell necrosis to apoptosis. Contrary to these two patients, antagomir 324 did not have any rescue effect after exposure to the third patient's serum. The exact reason for this is unknown, however, this patient possessed the lowest concentration of ALT which may have reflected a lesser liver injury and therefore lower toxic load to the cells (Supplementary Table 5).

In conclusion, we demonstrate that a novel miR inhibitor, antagomir 324, plays a major role in the regulation of SULT2A1, improving cell survival in the context of acute injury and patient recovery following paracetamol overdose. We believe that these studies are novel and offer serious promise to reduce the toxic effects of paracetamol overdose.

REFERENCES

Appleboam, AV., Dargan, PI., and Knighton, J (2002) Fatal anaphylactoid reaction to N-acetylcysteine: caution in patients with asthma. *Emergency Medicine Journal*. **19**(6): 594-595.

Baek, D., Villen, J., Shin, C *et al* (2008) The impact of microRNAs on protein output. *Nature*. **455** (7209): 64-71.

Bailey, B. and McGuigan, MA (1998) Management of anaphylactoid reactions to intravenous N-acetylcysteine. *Annals of Emergency Medicine*. **31**(6): 710-715.

Bari K., and Fontana, RJ (2014) Acetaminophen overdose: what practitioners need to know. *Clinical Liver Disease*. **4**(1): 17-21.

Bartel, DP (2009) MicroRNAs: target recognition and regulatory functions. *Cell.* **136**: 215-233.

Cameron, K., Tan, R., Schmidt-Heck, W *et al* (2015) Recombinant laminins drive the differentiation and self-organization of hESC-derived hepatocytes. *Stem Cell Reports*. **5**: 1-13.

Chun, LJ., Tong, MJ., Busuttil, RW., and Hiatt, JR (2009) Acetaminophen hepatotoxicity and acute liver failure. *Journal of Clinical Gastroenterology*. **43**(4): 342-349.

Craig DG, Lee P, Pryde EA, Hayes PC, Simpson KJ. Serum neopterin and soluble CD163 as markers of macrophage activation in paracetamol (acetaminophen)-induced human acute liver injury (2013). *Alimentary Pharmacology and Therapeutics* **38**:1395-1404

Daige, CL., Wiggins, JF., Priddy,L., Nelligan – Davis, T., Zhao, J., and Brown, D (2014) Systemic delivery of a miR-34a mimic as a potential therapeutic for liver cancer. *Molecular Cancer Therapeutics*. **13**(10): 2352-2360.

Davies, EC., Green, CF., Taylor, S., Williamson, PR., Mottram, DR., and Pirmohamed, M (2009) Adverse drug reactions in hospital in-patients: a prospective analysis of 3695 patient-episodes. *PLoS ONE*. **4**: e4439.

Davies, EC., Green, CF., Mottram, DR., Rowe, PH., and Pirmohamed, M (2010) Emergency re-admissions to hospital due to adverse drug reactions within 1 year of the index admission. *British Journal of Clinical Pharmacology*. **70**: 749-755.

Dollery, C (1993) Therapeutic Drugs; Volumes 1 and 2 Edition. London: Churchill Livingstone.

Fontana, RJ (2008) Acute liver failure including acetaminophen overdose. *Medical Clinics of North America*. **97**(4):761-794.

Friedman, RC., Farh, KK., Burge, CB., and Bartel, DP (2009) Most mammalian mRNAs are conserved targets of microRNAs. *Genome Research*. **19**:92-105.

Grimson, A., Farh, KK., Johnston, WK., Garrett – Engele, P., Lim, LP., and Bartel, DP (2007) MicroRNA targeting specificity in mammals: determinants beyond seed pairing. *Molecular Cell*. **27**:91-105.

Harrison, PM., Keays, R., Bray, GP *et al* (1990) Improved outcome of paracetamol-induced fulminant hepatic failure by late administration of acetylcysteine. *Lancet*. **335**: 1572-1573.

Hay, DC., Fletcher, J., Payne, C., *et al* (2008) Highly efficient differentiation of hESCs to functional hepatic endoderm requires Activin A and Wnt3a signalling. *Proc.Natl.Acad.Sci.USA*. **105**: 12301-12306.

Hay, DC., Pernagallo, S., Diaz-Mochon, JJ., *et al* (2011) Unbiased screening of polymer libraries to define novel substrates for functional hepatocytes with inducible drug metabolism. *Stem Cell Research*. **6**:92-102.

Heidet, L., and Gubler, MC (2009) The renal lesions of Alport Syndrome. *Journal of the American Society of Nephrology*. **20**(6): 1210-1215.

Hoofnagle, JH., Carithers, RL., Shapiro C. *et al* (1995) Fulminant hepatic failure: summary of a workshop. *Hepatology*. **21**: 240-252.

Jaeschke H, McGill MR, Ramachandran A. (2012) Oxidant stress, mitochondria, and cell death mechanisms in drug-induced liver injury: lessons learned from acetaminophen hepatotoxicity. *Drug Metabolism Reviews*. **44**(1):88-106.

Kalscheuer, S., Zhang, X., Zeng, Y *et al* (2008) Differential expression of microRNAs in early-stage neoplastic transformation in the lungs of F344 rats chronically treated with the tobacco carcinogen 4-(methylnitrosamino)-1—(3-pyridyl)-1-butanone. *Carcinogenesis*. **29**: 2394-2399.

Kovalchuk, O., Filkowski,J., Meservy, J *et al* (2008) Involvement of microRNA – 451 in resistance of the MCF-7 breast cancer cells to chemotherapeutic drug doxorubicin. *Molecular Cancer Therapeutics*. **7**:2152-2159.

Lewis, BP., Burge, CB., and Bartel, DP (2005) Conserved seed pairing, often flanked by adenosines, indicates that thousands of human genes are microRNA targets. *Cell*. **120**:15-20.

Liao, R., Sun, J., Zhang, L *et al* (2008) MicroRNAs play a role in the development of human hematopoietic stem cells. *Journal of Cellular Biochemistry*. **104**: 805-817.

Medine, CN., Lucendo –Villarin, B., Storck, C., Wang, F., Szkolnicka, D., Khan, F., Pernagallo, S., Black, JR., Marriage, HM., Ross, JA., Bradley, M., Iredale, JP., Flint, O., and Hay, DC (2013) Developing high-fidelity hepatotoxicity models from pluripotent stem cells. *Stem Cells Translational Medicine*. **2**(7): 505-509.

Nourjah, P., Ahmad, SR., Karwoski, C., and Willy, M (2006) Estimates of acetaminophen (paracetamol) – associated overdoses in the United States. *Pharmacoepidemiology and Drug Safety*. **15**(6): 398-405.

Olsen, AK., and Whalen, MD (2009) Public perceptions of the pharmaceutical industry and drug safety: implications for the pharmacovigilance professional and the culture of safety. *Drug Safety*. **32**: 805-810.

Pakravan, N., Waring, WS., Sharma, S *et al* (2008) Risk factors and mechanisms of anaphylactoid reactions to acetylcysteine in acetaminophen overdose. *Clinical Toxicology (Philadelphia, Pa)*. **46**(8): 697-702.

Pan, YZ., Gao, W., and Yu, AM (2009a) MicroRNAs regulate CYP3A4 expression via direct and indirect targeting. *Drug Metabolism and Disposition*. **37**: 2112-2117.

Pan, YZ., Morris, ME., and Yu, AM (2009b) MicroRNA-328 negatively regulates the expression of breast cancer resistance protein (BCRP/ABCG2) in human cancer cells. *Molecular Pharmacology*. **75**: 1374-1379.

Pirmohamed, M. (2004) Adverse drug reactions as cause of admission to hospital: prospective analysis of 18 820 patients. *BMJ*. **329**:15-19.

Polson, JP., Lee, WM. (2005) AASLD position paper: The management of acute liver failure. *Hepatology*. **41**: 1179-97.

Szkolnicka, D., Farnworth, SL., Lucendo-Villarin, B., Storck, C., Zhou, W., Iredale, JP., Flint,O., and Hay, DC (2014a) Accurate prediction of drug-induced liver injury using stem cell – derived populations. *Stem Cells Translational Medicine*. **3**(2): 141-148.

Szkolnicka, D., Farnoworth, SL., Lucendo-Villarin, B., and Hay, DC (2014b) Deriving functional hepatocytes from pluripotent stem cells. *Current Protocols in Stem Cell Biology*. **30**: 1G.5.1 – 1G.5.12

Thong, VD., Akkarathamrongsin, S., Poovorawan, K., Tangkijvanich, and Poovorawan, Y (2014) Hepatitis C virus genotype 6: virology, epidemiology, genetic variation and clinical implication. *World Journal of Gastroenterology*. **20**(11):2927-2940.

To KK., Zhan,Z., Litman, T *et al* (2008) Regulation of ABCG2 expression at the 3' untranslated region of its mRNA through modulation of transcript stability and protein translation by a putative microRNA in the S1 colon cancer cell line. *Molecular Cell Biology*. **28**: 5147-5167.

Tsuchiya, Y., Nakajima, M., Takagi, S *et al* (2006) MicroRNA regulates the expression of human cytochrome P450 1B1. *Cancer Research.* 66:9090-8.

Winek, CL (1994) Drug and chemical blood-level data. Winek's Toxicological Annual, Pitsburgh. Allegheny County Department Laboratories.

Witkos, TM., Koscianska, E., and Krzyzosiak, WJ (2011) Practical aspects if microRNA target prediction. *Current Molecular Medicine*. **11**: 93 – 109.

Yu, AM (2009) Role of microRNAs in the regulation of metabolism and disposition. *Expert Opinion on Drug Metabolism and Toxicology*. **5**(12): 1513-28.

Yu, X., Dhakal, IB., Beggs, M *et al* (2010) Functional genetic variants in the 3' untranslated region of sulfotransferase isoform 1A1 (SULT1A1) and their effect on enzymatic activity. *Toxicological Sciences*. **118** (2): 391-403.

Yu, AM., and Pan YZ (2012) Noncoding microRNAs: small RNAs play a big role in regulation of ADME? *Acta Pharmaceutica Sinica B*. **2**(2): 93-101.

Zhu, H., Wu,H., Liu,X *et al* (2008) Role of microRNA miR-27a and miR-451 in the regulation of MDR1/P-glycoprotein expression in cancer cells. *Biochemical Pharmacology*. **76**: 582-588.

FIGURE LEGENDS

Figure 1: Stagewise human embryonic stem cell (hESC) differentiation to the hepatocyte lineage. **(A)** Phase-constrast imaging demonstrated that cells underwent sequential morphological changes during transit from stem cell (day 0), to definitive endoderm (day 3), to hepatoblast (day 10), to hepatocyte (day 18). **(B)** Immunocytochemistry demonstrating upregulation of HNF4a and albumin during hepatic specification at day 18. Negative controls performed with corresponding immunoglobulin G (IgG). The percentage of positive cells is provided in the top right of each panel. This was calculated from four random fields of view and is quoted as ± standard error. **(C)** Cyp3A and Cyp1A2 metabolism were measured in day 18 hepatocyte like cells using the Promega pGlo system™. Experiments were performed in triplicate and measured on a luminometer. The units of activity quoted are relative light units per millilitre of supernatant per milligram of protein (RLU/mg/ml). The scale for all images represent 100 um. Abbreviations: HNF4a, hepatocyte nuclear factor 4a; ALB, Albumin.

Figure 2: Stem cell –derived (day 18) and primary human hepatocyte gene expression. The scatter plots represent expression of the major metabolic genes involved in Phase I, Phase II, and Phase III drug metabolism. Gene expression was performed using Human Drug Metabolism RT^2 Profiler PCR Array (QIAGEN) according to the manufacture**'s** instructions. The gene expression was analysed by RT2 Profiler PCR Array Data Analysis version 5.0 (QIAGEN). The scatter plot represents 3 fold change in gene expression. The graph plots the $\log_{10}$ of normalized gene expression levels in a control condition**, primary human hepatocytes** (x-axis) versus an experimental condition, **hESC-derived hepatocytes** (y-axis). Symbols outside the boundary area indicate fold –differences larger than a threshold (3 fold). The red symbols in the upper - left corner readily identify up-regulated genes, and the green symbols in the lower-right corner readily identify down-regulated genes. The human primary hepatocyte total RNA was purchased from 3H Biomedical (Sweden).

Figure 3: The expression of enzymes and transporters involved in paracetamol (APAP) metabolism. **(A)** The panel represents protein expression of phase II enzymes GSTT1, SULT2A1 and Phase III transporters ABCC1, ABCG2 in stem cell – derived hepatocytes. The percentage of positive cells is provided in the top right of each panel. This was calculated from four random fields of view and is quoted as ± standard error. The images were taken at x 20 magnification. Scale bar represents 100 um. **(B)** Phase II enzymes (GSTT1, SULT2A1) and Phase III transporters (ABCG2, ABCC1) play major role in a toxic and non-toxic

pathways of paracetamol metabolism. In the non-toxic pathway paracetamol is metabolised by SULT2A1 enzymes to produce APAP sulfate metabolite that is effluxed from the cell by ABCG2 transporter. In a toxic pathway, paracetamol is metabolised by GSTT1 enzyme to produce APAP cysteine (mercapturic acid) metabolite that is effluxed from the cell by ABCC1 transporter. Abbreviations: GSTT1, glutathione-S-transferase theta 1; SULT2A1, sulfotransferase 2A1; ABCG2, ATP-Binding Cassette Transporter Subfamily G member 2; ABCC1, ATP-Binding Cassette Transporter Subfamily C member 1.

Figure 4: hESC-derived hepatocytes (hESC-heps) and primary human hepatocytes (PHH) microRNA expression profile. **(A)** Principle Component Analysis overview plot demonstrates strong clustering by cell type. **(B)** Statistical analysis of the microRNA Array demonstrates 367-reliably detected microRNAs in both hESC-heps and PHH; 220 microRNAs have a similar expression in both systems, and 147 microRNAs are differentially-expressed. **(C)** microRNA 122 (miR-122) is expressed in hESC-heps at the same level as in PHH. The microRNA Array was carried out by Sistemic **Limited**. The RNA samples (4 replicates of PHH and 4 experimental samples of hESC-derived hepatocytes) were run on Agilent miRNA platform.

Figure 5: Antagomir of microRNA 324 upregulated SULT2A1 gene and protein expression and increased cell survival after exposure to paracetamol. At day 17, hESC-heps were transfected with the antagomir of the corresponding microRNA at 50 nM for 24 hours. Transfection with the Ant-324-5p upregulated SULT2A1 gene expression by 2-fold **(A)** and protein expression by 20% **(B)** in comparison with the scrambled control. At day 17, hESC-hepatocytes were either transfected with antagomirs or treated with **1 mM N-acetylcysteine** (NAC) concentration for 24 hours. At day 18, the the antagomir transfected or NAC pre-exposed hESC-hepatocytes were exposed to paracetamol concentration that causes 50% of the cell death (IC50 = 12.85 mM) for another 24 hours. At day 19, the cell viability was measured using CellTitre Assay (Promega) and Glutathione Depletion Assay (Promega). The antagomir of microRNA 324 (Ant 324) significantly increased ATP to the levels comparable with NAC (fold increase was calculated in comparison with control; the values for Ant ctrl = 2.17 x 10^8; Ant 324= 3.12 x 10^8; H_2O (vehicle) = 2.38 x 10^8; NAC = 3.86 x 10^8 **(C)** and enhanced reduced glutathione levels **(D)**. Levels of significance were measured by Student's t test. Significance levels are denoted by one asterisks to indicate $p < 0.05$. The percentage of positive cells is provided in the top right of each panel. This was calculated from four random fields of view and is quoted as ± standard error. The scale bar represents: 100 um.

Abbreviations: SULT2A1, sulfotransferase 2A1; Ant Control; Scrambled Antagomir Control; Ant 324; Antagomir 324-5p. Levels of significance were measured by Student's t test. Significance levels are denoted by one asterisk to indicate $p < 0.05$.

Figure 6: hESC-derived hepatocytes transfected with the antagomir to miR-324-5p. Twenty four hours post transfection hESC-hepatocytes were exposed to the plasma from patients with fulminant hepatic failure for a further twenty four hours (Patients 1, 8 and 58). ATP levels and caspase 3/7 activation were determined using Promega Glo technology and measured on a luminometer (Promega). Units of activity are expressed as relative light units (RLU) ml^{-1} (n=4). Levels of significance are quoted and measured by Student's *t*-test. Significance levels are denoted by one and two asterisks to indicate $p < 0.05$ and $p < 0.01$ respectively.

Supplementary Figure 1: Metabolic activity of female and male primary human hepatocytes. Cyp3A and Cyp1A2 metabolism were measured in both lines 48 hours post-replating using the Promega pGlo system™. Experiments were performed in triplicate and measured on a luminometer. The units of activity quoted are relative light units per millilitre of supernatant per milligram of protein (RLU/mg/ml).

Supplementary Figure 2: Paracetamol (APAP) metabolism (based on Pharmacogenomics Knowledge Base PharmGKB; www.pharmgkb.org). At normal doses APAP is metabolised by two major families of phase II enzymes: Sulfotransferases (SULTs) and UDP-glucuronosylltransferases (UGTs). This leads to the production of two metabolites: APAP-sulfate and APAP-glucuronide, which are further effluxed from the cell by one of the ABC transporters. At higher doses than recommended, paracetamol is metabolised by Cytochrome P450 enzymes. This leads to the formation of a reactive metabolite, N-acetyl-p-benzoquinoneimine (NAPQI), which is further transformed to a non-toxic APAP- cysteine by Glutathione –S- transferases (GSTT1,GSTP1). The metabolite is effluxed from the cell by one of the phase III transporters.

Supplementary Figure 3: Paracetamol *in vitro* toxicity in stem-cell derived hepatocytes (hESC-heps) and primary human hepatocytes (PHH). hESC-heps (at day 17) and PHH (24 hours post- replating) were induced with different concentrations of paracetamol (0-50 mM) for 24 hours. The CellTitre viability assay (Promega) was used to measure the ATP levels. The IC50 was calculated from the function $f(x)= ax + b$.

Supplementary Figure 4: At day 17, hESC-heps were transfected with the antagomir of the corresponding microRNA at 50 nM concentration for 24 hours. Transfection with the antagomir of microRNA 24-3p did not have any effect either on gene **(A)** or protein **(B)** expression of GSTT1. At day 18, the transfected hESC-heps were exposed to paracetamol concentration that causes 50% of the cell death (IC50 = 12.85 mM) for another 24 hours. At day 19, the cell viability was measured using CellTitre Assay (Promega) and Glutathione Depletion Assay (Promega). The Ant-24 decreased cell viability **(C)** and reduced glutathione **(D)** after exposure to paracetamol comparing to the scrambled control. The percentage of positive cells is provided in the top right of each panel. This was calculated from four random fields of view and is quoted as ± standard error. The scale bar represents: 100 um. Abbreviations: Ant Control; Scrambled Antagomir Control; Ant 324; Antagomir 324-5p.

Supplementary Figure 5: At day 17, hESC-derived hepatocytes were transfected with precursors at 50nM concentration for 24 hours. At day 18, cells were exposed to paracetamol (APAP) concentration that causes 50% of the cell death (IC50 = 12.85 mM) for 24 hours. At day 19, the cell viability and glutathione reduction were measured using CellTiter – Glo® Luminescent Cell Viability Assay (Promega) and GSH/GSSG – Glo™ Assay (Promega) respectively. Abbreviations: Pre; precursor. Pre ctrl/Pre 24/Pre 324, precursor scrambled control/ precursor of miR -24/ precursor of miR -324-5p. Levels of significance are quoted and measured by Student's *t*-test. Significance levels are denoted by one asterisks to indicate $p < 0.05$.

Supplementary Table 1: Fold-Change (2^(- Delta Delta Ct)) is the normalized gene expression (2^(- Delta Ct)) in the Test Sample divided the normalized gene expression (2^(- Delta Ct)) in the Control Sample. Fold-Regulation represents fold-change results in a biologically meaningful way. Fold-change values greater than one indicate a positive- or an up-regulation, and the fold-regulation is equal to the fold-change. Fold-change values less than one indicate a negative or down-regulation, and the fold-regulation is the negative inverse of the fold-change. Up-regulated genes (fold differences larger than a 3 fold threshold) are indicated in red, down-regulated genes (fold differences narrower than 3 fold treshold) are indicated in green. Genes similarly expressed for the Group 1 and Control (fold differences between -3 to +3 boundary) are indicated in black. Abbreviations: HLC, hepatocyte-like-cells; PHH, primary human hepatocytes.

Supplementary Table 2: The list of 220 microRNAs commonly expressed in stem cell – derived hepatocytes (day 18) and primary human hepatocytes (PHH). The RNA samples (4 replicates of PHH and 4 experimental samples of hESC-derived hepatocytes) were analysed on the Agilent miRNA platform (using Agilent's SurePrint G3 Human v16 microRNA 8x60K microarray slides; miRBase version 16.0.

Supplementary Table 3: Predicted microRNA/mRNA binding site by TargetScanHuman5.2 (www.targetscan.com). **(A)** Human microRNA hsa-miR-324-5p has been predicted to bind its target gene SULT2A1 at the 3' untranslated region at position between 639-645 nt. Human microRNA has-miR-24-3p has been predicted to bind its target gene GSTT1 at the 3' untranslated region at position between 266-272 nt. **(B)** The table represents type of seed match and context score for each of the microRNA/mRNA binding. **(C)** The table represents the miRBase accession number of each of the selected microRNAs and UniGene and GeneBank of selected genes of interest. Abbreviations: SULT2A1, sulfotransferase 2A1; GSTT1, glutathione-s-transferase theta 1.

Supplementary Table 4: The table demonstrates qPCR primers, and primary/secondary antibodies used in this study.

Supplementary Table 5: Anonymised patient details. (A) The table represents the plasma contents of each of the patients used in this study. (B) The table represents normal ranges for particular sera and international normalized ratio (INR). **ALT and BILI are liver function tests. Creatinine is a measure of renal function, which is often compromised in liver disease INR is International Normalized Ratio of the prothrombin time, a coagulation function test.**

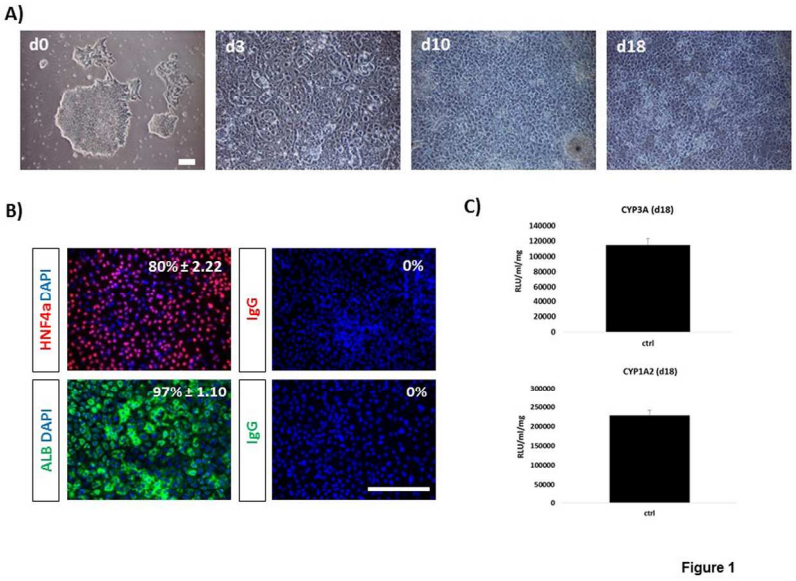

Figure 1

400x235mm (200 x 200 DPI)

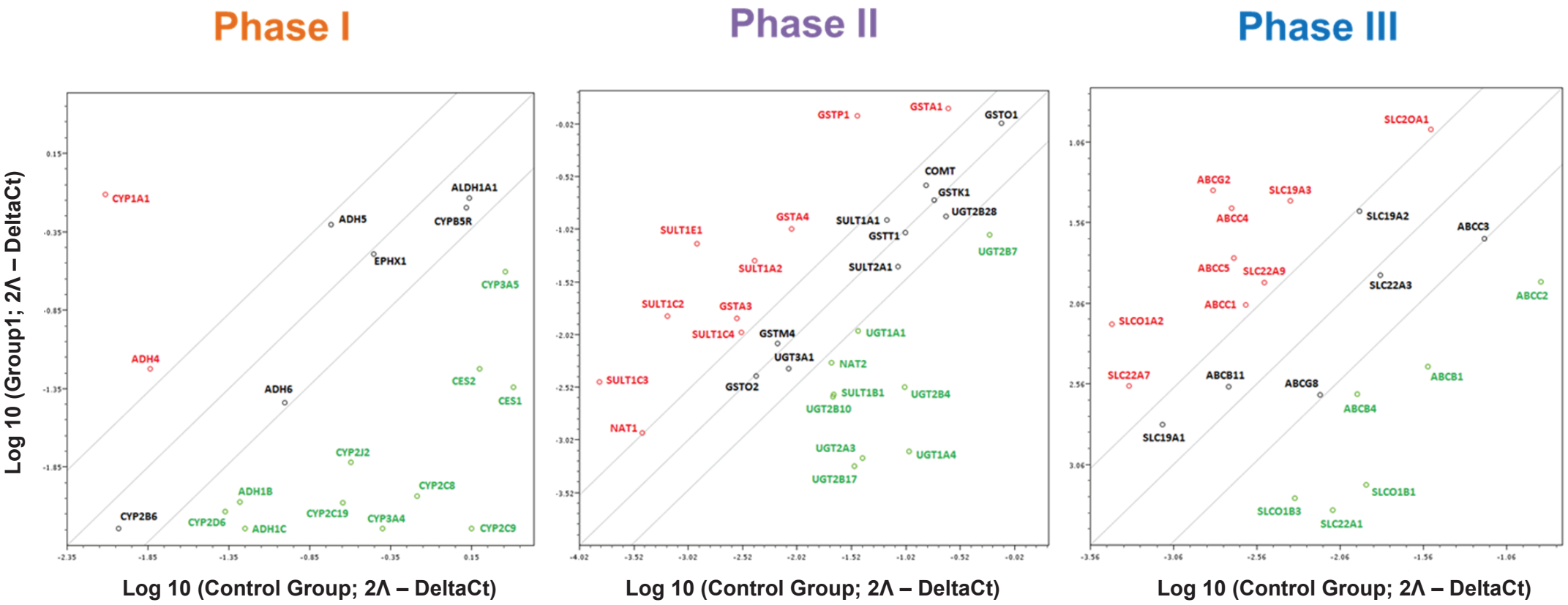

Increased Decreased Similar

Figure 2

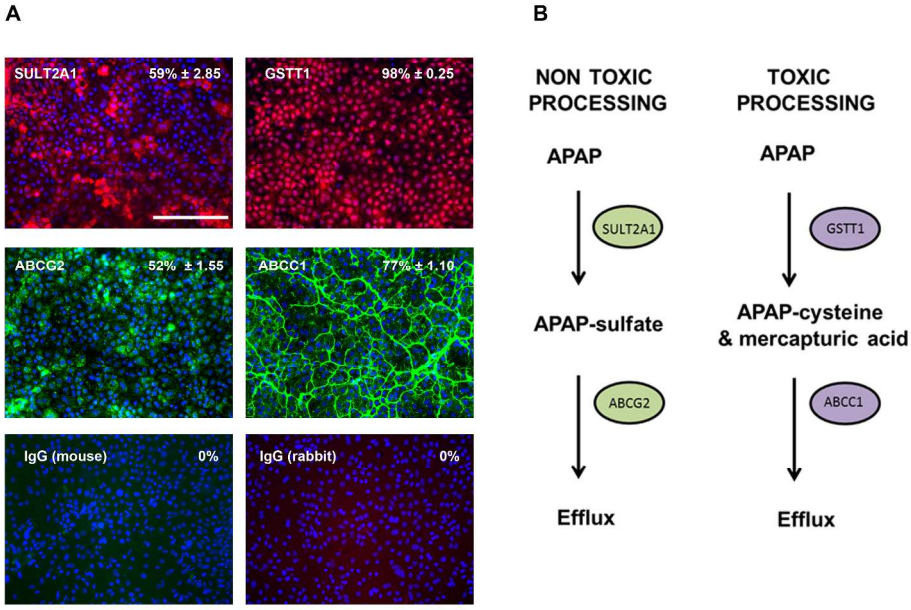

Figure 3

297x209mm (300 x 300 DPI)

A

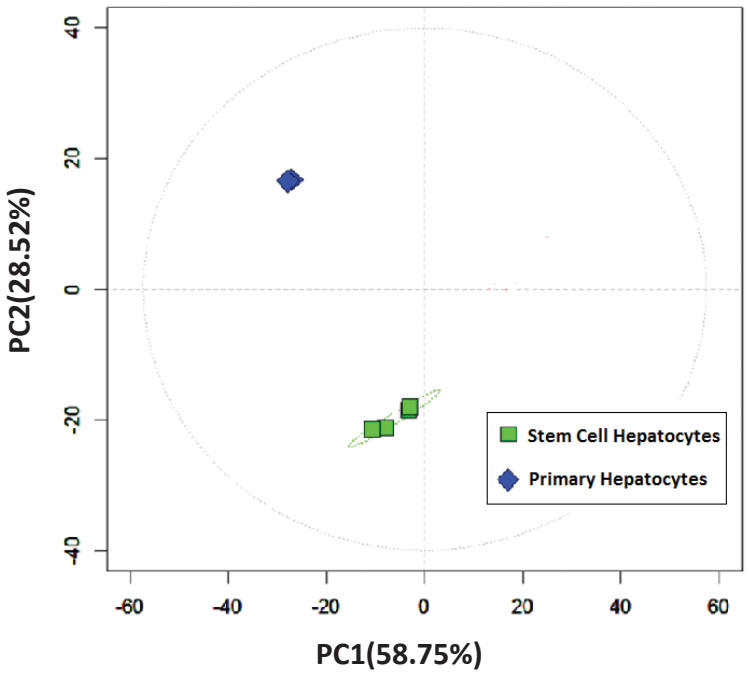

C

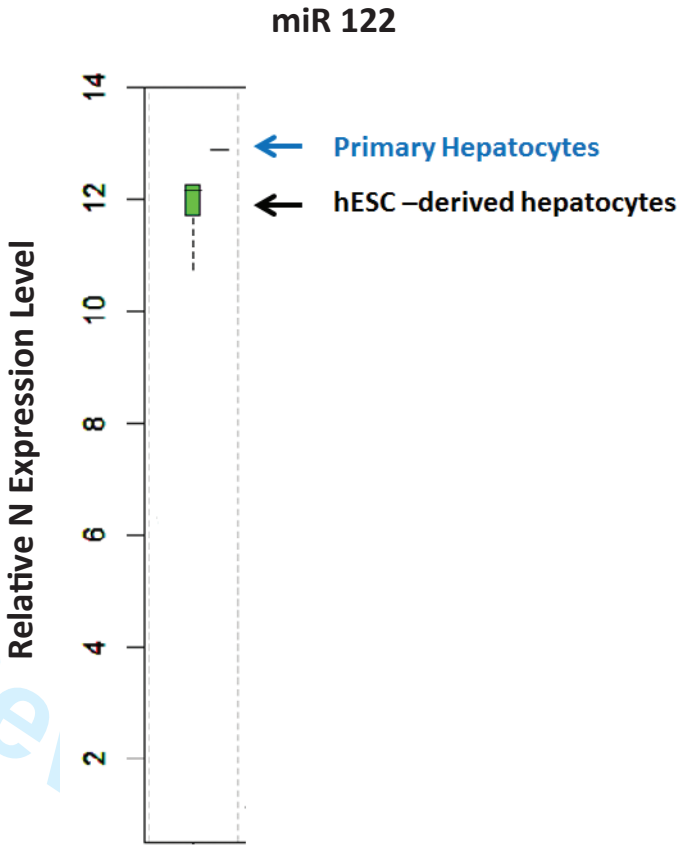

B

Primary Hepatocytes versus hESC- derived hepatocytes	
Total (common) number of expressed miRs	367
Number of the same miRs	220 (60 %)
Number of differentially-expressed miRs	147 (40 %)

Figure 4

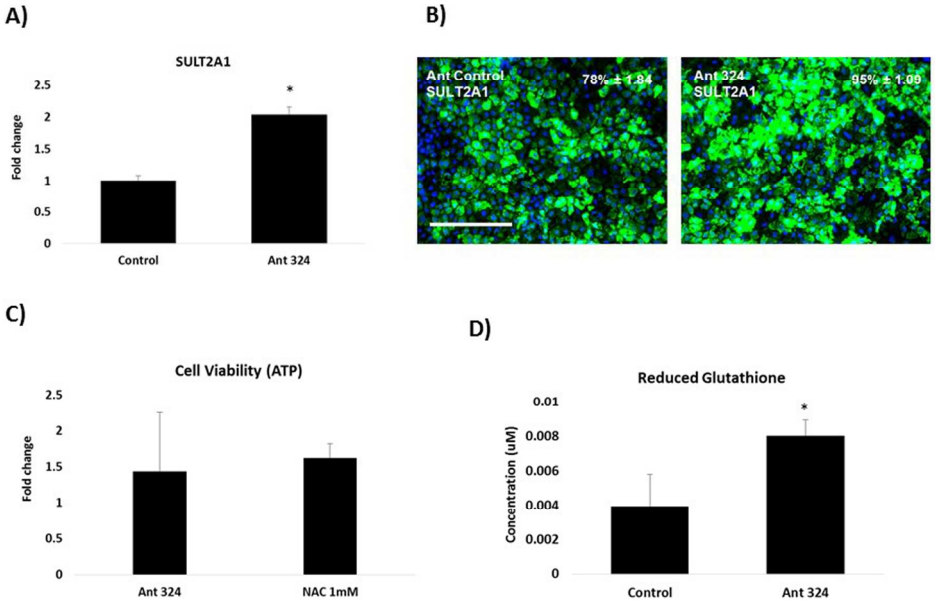

Figure 5

254x190mm (200 x 200 DPI)

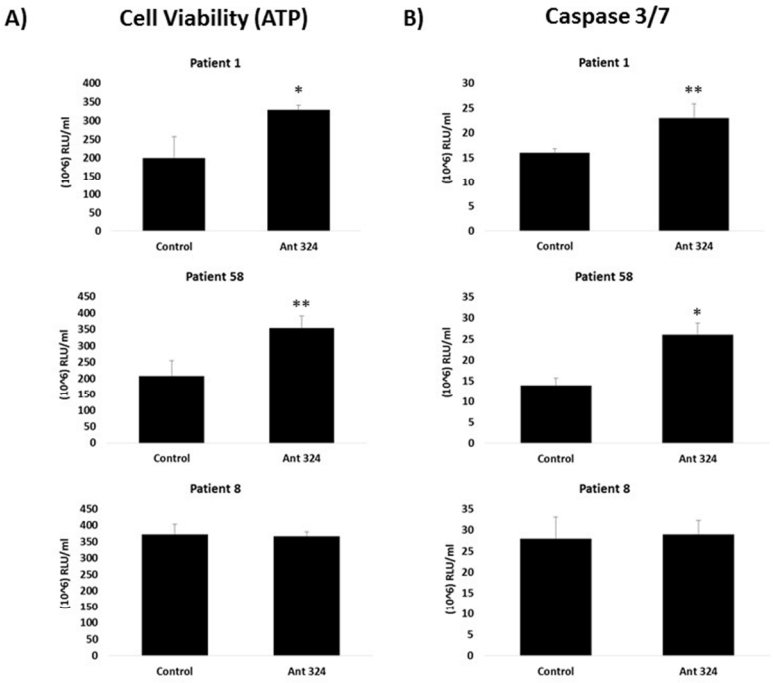

Figure 6

254x190mm (96 x 96 DPI)

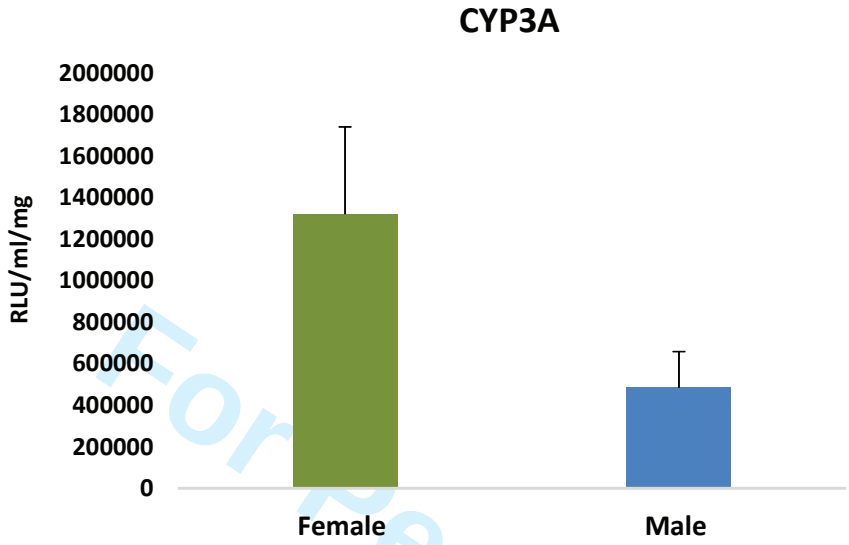

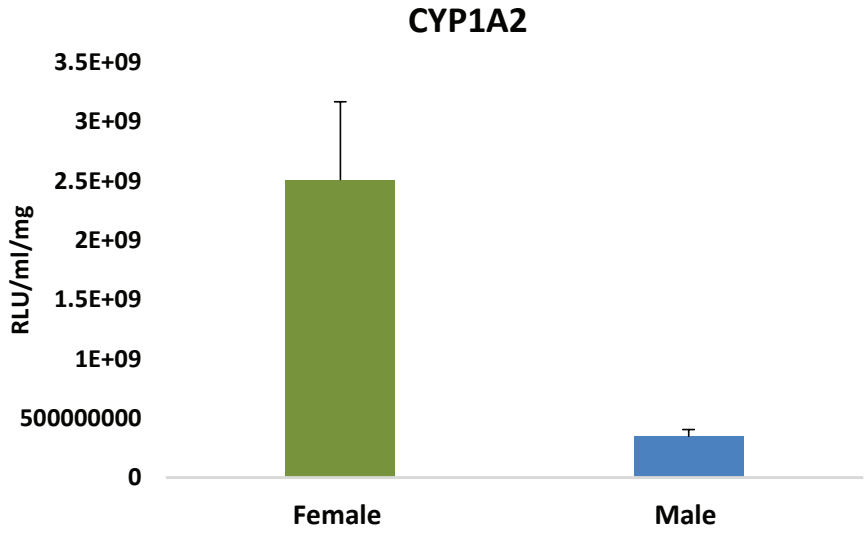

Supplementary Figure 1

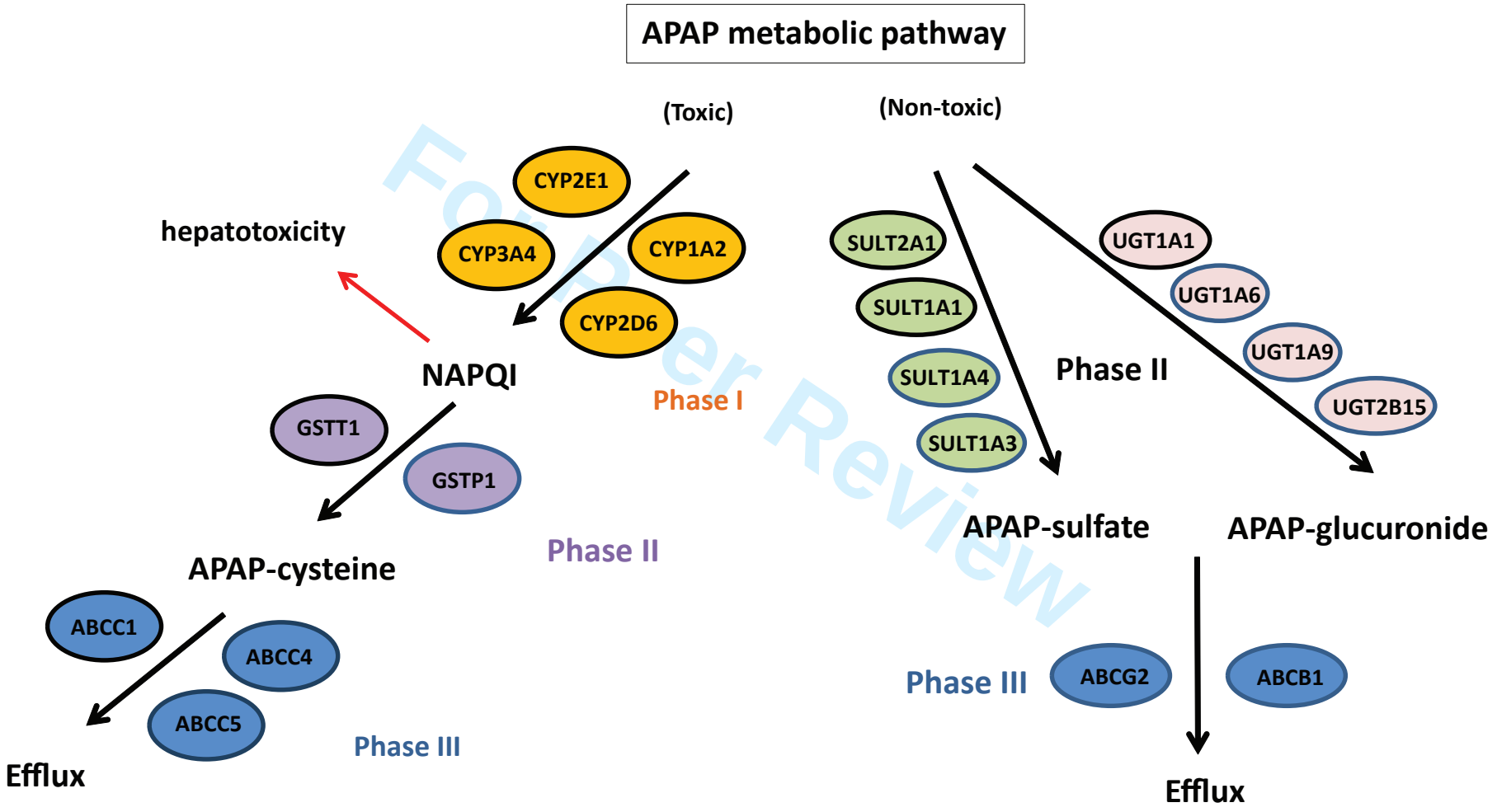

Supplementary Figure 2

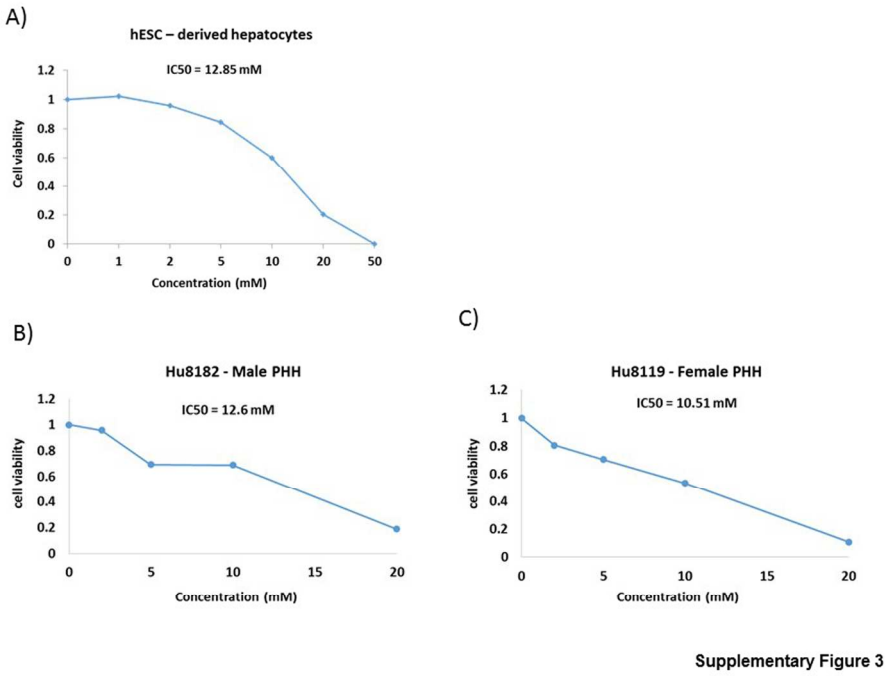

Supplementary Figure 3

400x299mm (200 x 200 DPI)

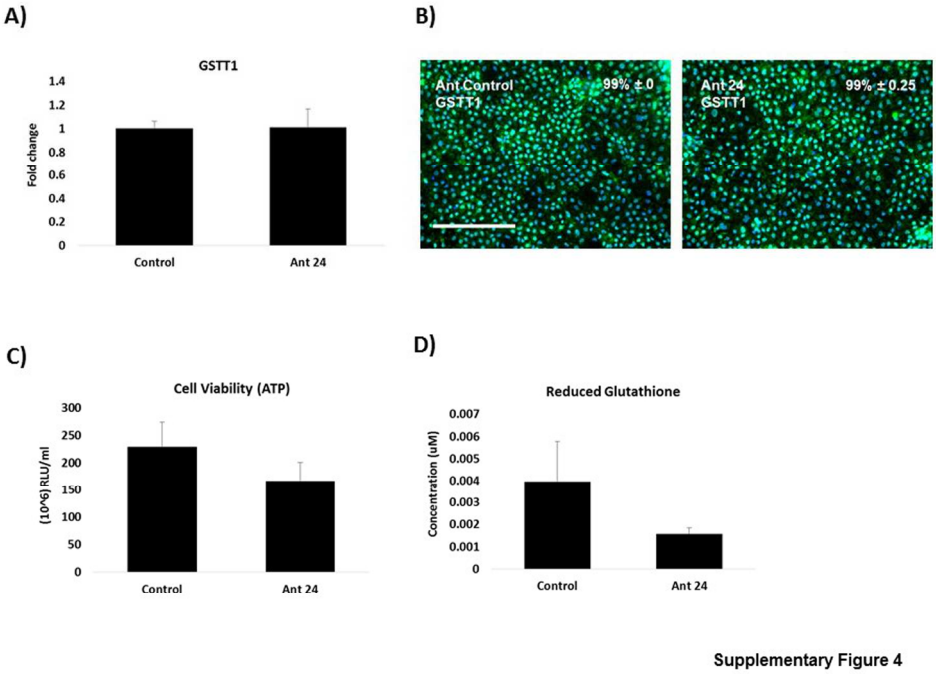

Supplementary Figure 4

400x299mm (200 x 200 DPI)

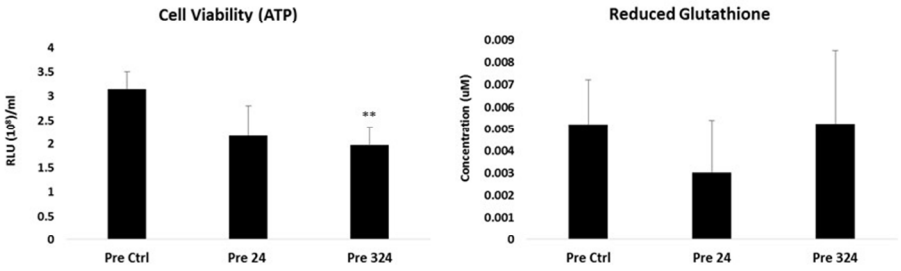

Supplementary Figure 5

254x190mm (96 x 96 DPI)

Supplementary Table 1

RT² PROFILER PCR ARRAY - Human Drug Metabolism Phase I (QIAGEN; PAHS-002Z)						
Gene Symbol	AVG ΔCt		2^ - ΔCt		Fold Change	Fold Up – or Down-Regulation
	Group1 (HLC)	Control Group (PHH)	Group1 (HLC)	Control Group (PHH)	Group 1/ Control	Group 1/ Control
CYP1A1	0.38	7.02	0.768483	0.007705	99.74	99.74
ADH4	4.08	6.10	0.059302	0.014562	4.07	4.07
ADH5	1.01	2.39	0.495439	0.190431	2.60	2.60
EPHX1	1.64	1.52	0.321538	0.347956	0.92	-1.08
ADH6	4.78	3.34	0.036387	0.098713	0.37	-2.71
ALDH1A1	0.45	-0.45	0.729565	1.363349	0.54	-1.87
CYPB5R	0.65	-0.38	0.636322	1.303635	0.49	-2.05
CYP2B6	7.46	6.75	0.005694	0.009309	0.61	-1.63
CYP3A5	2.01	-1.18	0.248204	2.272074	0.11	-9.15
CYP2J2	6.06	1.98	0.015040	0.252693	0.06	-16.80
CYP2C8	6.76	0.63	0.009224	0.647110	0.01	-70.16
CYP2C9	7.46	-0.49	0.005694	1.402808	0.00	-246.36
CYP3A4	7.46	1.34	0.005694	0.394672	0.01	-69.31
CYP2C19	6.91	2.15	0.008323	0.225670	0.04	-27.11
CYP2D6	7.09	4.56	0.007318	0.042426	0.17	-5.80
CES1	4.46	-1.36	0.045546	2.559360	0.02	-56.19
CES2	4.07	-0.66	0.059552	1.579842	0.04	-26.53
ADH1B	6.89	4.26	0.008442	0.052291	0.16	-6.19
ADH1C	7.46	4.16	0.005694	0.056056	0.10	-9.84

RT² PROFILER PCR ARRAY - Human Drug Metabolism Phase II (QIAGEN; PAHS-069Z)						
Gene Symbol	AVG ΔCt		2^ - ΔCt		Fold Change	Fold Up – or Down-Regulation
	Group1 (HLC)	Control Group (PHH)	Group1 (HLC)	Control Group (PHH)	Group 1/ Control	Group 1/ Control
GSTP1	-0.20	4.85	1.148277	0.034646	33.14	33.14

Supplementary Table 1

GSTA1	-0.42	2.08	1.341208	0.236264	5.68	5.68
GSTA4	3.37	6.86	0.096681	0.008588	11.26	11.26
GSTA3	6.20	8.55	0.013622	0.002677	5.09	5.09
SULT1E1	3.85	9.74	0.069583	0.001166	59.66	59.66
SULT1A2	4.37	7.98	0.048511	0.003948	12.29	12.29
SULT1C2	8.20	12.73	0.003411	0.000147	23.14	23.14
SULT1C3	8.20	12.73	0.003411	0.000147	23.14	23.14
SULT1C4	6.63	8.40	0.010075	0.002967	3.40	3.40
NAT 1	9.80	11.43	0.001118	0.000362	3.09	3.09
GSTO1	0.04	0.46	0.971041	0.724547	1.34	1.34
GSTO2	8.00	7.95	0.003893	0.004040	0.96	-1.04
GSTT1	3.47	3.39	0.089944	0.095282	0.94	-1.06
GSTK1	2.45	2.52	0.182812	0.174788	1.05	1.05
GSTM4	6.98	7.30	0.007905	0.006338	1.25	1.25
UGT2B28	2.98	2.15	0.126827	0.225954	0.56	-1.78
UGT3A1	7.78	6.94	0.004559	0.008118	0.56	-1.78
SULT1A1	3.08	3.96	0.117951	0.064148	1.84	1.84
SULT2A1	4.55	3.61	0.042611	0.081891	0.52	-1.92
COMT	2.01	2.76	0.249051	0.147120	1.69	1.69
UGT1A1	6.58	4.83	0.010486	0.035145	0.30	-3.35
UGT1A4	10.39	3.28	0.000746	0.102607	0.01	-137.61
UGT2B4	8.36	3.41	0.003054	0.093826	0.03	-30.73
UGT2B7	3.56	0.83	0.084852	0.564152	0.15	-6.65
UGT2B10	8.65	5.59	0.002489	0.020726	0.12	-8.33
UGT2A3	10.59	4.69	0.000649	0.038640	0.02	-59.49
UGT2B17	10.85	4.95	0.000543	0.032289	0.02	-59.46
NAT2	7.58	5.64	0.005230	0.020051	0.26	-3.83
SULT1B1	8.60	5.59	0.002579	0.020766	0.12	-8.05

RT^2 PROFILER PCR ARRAY - Human Drug Transporters Phase III (QIAGEN; PAHS-070Z)						
Gene Symbol	**AVG ΔCt**		**2^ - ΔCt**		**Fold Change**	**Fold Up – or Down-Regulation**
	Group1 (HLC)	**Control Group (PHH)**	**Group1 (HLC)**	**Control Group (PHH)**	**Group 1/ Control**	**Group 1/ Control**
ABCC1	6.89	8.73	0.008423	0.002350	3.58	3.58
ABCC4	4.89	9.01	0.033689	0.001934	17.42	17.42
ABCC5	5.93	8.98	0.016410	0.001982	8.28	8.28
ABCG2	4.52	9.39	0.043502	0.001491	29.17	29.17
SLCO1A2	7.29	11.41	0.006390	0.000368	17.38	17.38
SLCO2A1	6.64	12.26	0.009994	0.000204	49.01	49.01
SLC19A3	4.75	7.85	0.037173	0.004328	8.59	8.59
SLC22A7	8.55	11.07	0.002659	0.000466	5.70	5.70
SLC22A9	6.43	8.37	0.011561	0.003030	3.82	3.82
ABCC3	5.53	3.98	0.021683	0.063471	0.34	-2.93
ABCB11	8.58	9.07	0.002616	0.001859	1.41	1.41
ABCG8	8.74	7.25	0.002338	0.006587	0.35	-2.82

Supplementary Table 1

SLC19A1	9.35	10.40	0.001529	0.000738	2.07	2.07
SLC19A2	4.95	6.46	0.032350	0.011345	2.85	2.85
SLC22A3	6.28	6.05	0.012855	0.015105	0.85	-1.18
ABCB1	8.16	5.09	0.003490	0.029260	0.12	-8.38
ABCB4	8.73	6.51	0.002351	0.011003	0.21	-4.68
ABCC2	6.42	2.84	0.011709	0.139434	0.08	-11.91
SLCO1B1	10.59	6.34	0.000648	0.012367	0.05	-19.09
SLCO1B3	10.88	7.76	0.000532	0.004626	0.12	-8.69
SLC22A1	11.12	7.00	0.000448	0.007829	0.06	-17.46

MICRORNAs COMMONLY EXPRESSED IN PRIMARY HUMAN HEPATOCYTES AND hESC - DERIVED HEPATO

miRNA	Mean log2 intensity	Relative mean intensity (%)	Max. log2 intensity
hsa-let-7b-3p	2.167553914	15.39758566	4.759083184
hsa-let-7e-5p	4.315044314	30.65264676	5.195762764
hsa-let-7f-1-3p	1.45060131	10.30459164	3.752587461
hsa-miR-1	1.562493903	11.09943959	4.033989956
hsa-miR-107	8.445884654	59.99676945	9.20038125
has-miR-1202	6.624326485	47.05702306	9.080396756
hsa-miR-1207-5p	8.276057831	58.79037591	10.36982484
hsa-miR-122-5p	10.08319276	71.62766441	12.88839682
hsa-miR-1224-5p	4.619021262	32.8119984	6.317471652
hsa-miR-1225-3p	3.997769591	28.39883213	5.235933105
hsa-miR-1225-5p	7.302618353	51.87538401	9.080396756
hsa-miR-1226*	2.73590075	19.4349335	6.432835079
hsa-miR-1228-3p	4.737513176	33.65372574	6.047606994
hsa-miR-1228-5p	2.336520334	16.59786719	5.533498506
hsa-miR-1234	5.018803171	35.65191678	6.517331819
hsa-miR-1237	3.113032203	22.11395052	4.222428371
hsa-miR-1238	4.283605841	30.42931826	5.402617074
hsa-miR-1246	9.203731352	65.38026159	12.88839682
hsa-miR-1249	1.710712988	12.15233891	3.779902166
hsa-miR-1258	1.366140729	9.704611618	3.652512778
hsa-miR-125a-3p	3.718808154	26.4171824	5.533498506
hsa-miR-125b-5p	6.907149701	49.06610558	8.24897089
hsa-miR-126-3p	4.453699943	31.63761046	6.745973602
hsa-miR-1260b	8.739559616	62.08293919	9.951193434
hsa-miR-1268b	6.897900491	49.00040226	8.914241059
hsa-miR-1275	7.082825486	50.31404822	9.543230472
hsa-miR-128	4.867008714	34.57361919	5.863396753
hsa-miR-1281	4.906137632	34.85157807	7.000447289
hsa-miR-1288	3.126365697	22.20866726	4.382662349
hsa-miR-1290	6.649179186	47.23356842	9.685937919
hsa-miR-1296	1.866800635	13.2611339	3.836693986
hsa-miR-1305	4.957477645	35.21628054	6.488825654
hsa-miR-133b	1.767910763	12.55865298	4.191590285
hsa-miR-135a-3p	3.580095563	25.43181406	5.333142011
hsa-miR-140-5p	3.713856714	26.38200901	5.333142011
hsa-miR-1471	2.371194554	16.84418138	5.108433596
hsa-miR-148a-3p	7.715908631	54.81126137	9.34381318
hsa-miR-148b-3p	5.16186919	36.66821043	6.317471652
hsa-miR-150-3p	4.834592275	34.34334353	7.181437537
hsa-miR-151a-3p	4.160489957	29.55474376	5.468096887
hsa-miR-151a-5p	6.759415776	48.01665268	7.908331533
hsa-miR-155-5p	2.817584404	20.01518714	4.174217694
hsa-miR-16-5p	8.507873725	60.4371193	9.685937919
hsa-miR-17-3p	3.717872965	26.41053913	5.605092098
hsa-miR-181a-5p	6.125048032	43.51031416	7.000447289

hsa-miR-181b-5p	4.149834728	29.47905254	4.97754762
hsa-miR-1825	4.717609699	33.51233803	6.609645511
hsa-miR-183-5p	3.26200335	23.17219225	5.2540446
hsa-miR-185-5p	3.599703802	25.5711045	4.964394851
hsa-miR-186-5p	3.107641947	22.07565993	4.576235395
hsa-miR-188-5p	5.832657074	41.43326556	9.2666837
hsa-miR-1909-5p	1.881355523	13.36452701	4.082699416
hsa-miR-191-3p	4.106883242	29.1739394	4.949522624
hsa-miR-1910	1.56203899	11.09620803	4.204958561
hsa-miR-1914-3p	4.204836624	29.8697678	5.120226753
hsa-miR-1915	8.285328163	58.85622928	10.65447387
hsa-miR-193a-5p	4.085079479	29.01905268	5.605092098
hsa-miR-197-3p	5.426277098	38.5464767	7.888192297
hsa-miR-1973	5.804181369	41.23098357	6.891326276
hsa-miR-198	2.236101149	15.88452253	5.2540446
hsa-miR-203	3.126895637	22.21243177	4.798541198
hsa-miR-205-3p	1.96851625	13.98368797	4.713406887
hsa-miR-20a-3p	2.765103481	19.64238003	4.366871399
hsa-miR-21-5p	12.09963664	85.95181434	12.88839682
hsa-miR-210	5.877366952	41.75086974	8.351444508
hsa-miR-211-5p	1.376709151	9.779686194	3.768765425
hsa-miR-218-5p	4.947405224	35.14472939	7.814426908
hsa-miR-22-5p	2.71668992	19.29846611	4.156098562
hsa-miR-221-3p	4.988289183	35.43515551	6.047606994
hsa-miR-224-5p	4.216325184	29.95137874	5.863396753
hsa-miR-2276	2.831064559	20.1109457	5.567690079
hsa-miR-23a-3p	8.369316464	59.45285437	9.2666837
hsa-miR-23b-3p	7.84616685	55.73657265	9.20038125
hsa-miR-24-3p	8.311629805	59.04306744	9.166945457
hsa-miR-25-3p	6.685005927	47.48806973	8.159537635
hsa-miR-26a-5p	7.010850118	49.80275903	8.782112163
hsa-miR-26b-5p	7.887656757	56.03130322	9.20038125
hsa-miR-27a-3p	7.070116486	50.22376769	8.24897089
hsa-miR-27b-3p	7.760195925	55.12586365	9.34381318
hsa-miR-28-5p	4.614680979	32.78116647	6.020154252
hsa-miR-2861	8.098232261	57.52716191	11.77690063
hsa-miR-30a-3p	2.950765003	20.96125804	4.534663185
hsa-miR-30a-5p	6.145492589	43.65554553	7.458327192
hsa-miR-30b-5p	6.546012759	46.50070827	7.941037626
hsa-miR-30c-5p	4.341174699	30.83826837	5.716816843
hsa-miR-30e-3p	2.959039546	21.02003765	4.481761629
hsa-miR-30e-5p	5.432525493	38.59086323	6.891326276
hsa-miR-31-3p	1.917007372	13.61778595	3.803379697
hsa-miR-31-5p	2.482850148	17.63734577	5.235933105
hsa-miR-3124-5p	1.762034727	12.51691157	4.011269468
hsa-miR-3125	3.744020805	26.59628473	5.090800321
hsa-miR-3127-5p	3.293369985	23.39501045	5.834190844
hsa-miR-3137	2.024382356	14.38054229	4.097587661
hsa-miR-3138	2.135530188	15.17009971	4.393786163

hsa-miR-3141	5.767174081	40.96809605	8.494581071
hsa-miR-3148	2.369747636	16.83390295	4.222428371
hsa-miR-3156-5p	2.410880989	17.12610068	4.964394851
hsa-miR-3162-5p	8.079116607	57.39137063	9.428341899
hsa-miR-3189-3p	1.562705153	11.10094023	3.595719016
hsa-miR-3191-5p	1.925673313	13.67934593	4.011269468
hsa-miR-3194-5p	1.967760055	13.97831621	3.966179414
hsa-miR-3195	6.693009447	47.54492409	8.629280443
hsa-miR-3196	6.794186938	48.2636555	8.739987987
hsa-miR-3198	5.172946014	36.74689652	6.457343715
hsa-miR-32-5p	2.221762751	15.7826673	3.814202968
hsa-miR-320a	6.064389577	43.07941657	8.039474417
hsa-miR-320b	7.151715081	50.80341711	9.20038125
hsa-miR-320c	8.230368171	58.46581168	9.951193434
hsa-miR-320d	7.725435848	54.87893956	9.428341899
hsa-miR-320e	7.356786278	52.26017503	9.166945457
hsa-miR-324-3p	5.300069944	37.64994285	6.488825654
hsa-miR-324-5p	4.49681939	31.94391675	5.468096887
hsa-miR-331-3p	7.044867749	50.04440902	8.494581071
hsa-miR-338-3p	2.500761434	17.76458161	3.872137461
hsa-miR-33a-5p	2.095408822	14.8850908	3.752587461
hsa-miR-340-5p	4.307660302	30.60019318	5.628631779
hsa-miR-342-3p	5.312297351	37.7368023	6.891326276
hsa-miR-345-5p	2.022335691	14.36600346	5.307697101
hsa-miR-3529-3p	3.279464699	23.2962319	4.97754762
hsa-miR-3610	2.916603406	20.71858536	6.233434393
hsa-miR-3613-3p	1.833489088	13.0244997	4.481761629
hsa-miR-362-3p	3.732515475	26.51455467	5.333142011
hsa-miR-362-5p	3.063632943	21.76303453	5.287277176
hsa-miR-3620	1.916020994	13.61077905	4.268604247
hsa-miR-3646	2.378256536	16.89434736	5.487612049
hsa-miR-3651	5.96417265	42.36750869	9.34381318
hsa-miR-3653	4.365243802	31.00924731	6.457343715
hsa-miR-3656	6.79527371	48.27137557	10.20739641
hsa-miR-365b-3p	7.351961072	52.22589835	8.449858467
hsa-miR-3665	9.552278389	67.85622439	12.88839682
hsa-miR-3667-5p	3.284815365	23.33424126	8.004693565
hsa-miR-3676-3p	3.64853392	25.9179775	4.602704884
hsa-miR-3679-5p	6.597281304	46.86490304	9.428341899
hsa-miR-3692-5p	1.749766601	12.42976285	4.393786163
hsa-miR-3713	1.783968337	12.67272067	3.779902166
hsa-miR-374a-5p	6.637281637	47.14905217	8.307345268
hsa-miR-375	2.79980384	19.8888799	4.314074629
hsa-miR-3917	1.810940875	12.86432465	3.562103075
hsa-miR-3935	2.140621	15.20626315	4.964394851
hsa-miR-3937	2.033564882	14.44577192	4.109507663
hsa-miR-3940-3p	1.514500304	10.75850894	3.814202968
hsa-miR-422a	2.052950141	14.58347839	4.314074629
hsa-miR-423-3p	2.172437369	15.43227611	3.652512778
hsa-miR-423-5p	5.293541426	37.60356641	6.81014592

hsa-miR-425-3p	3.884924864	27.59722053	5.143929899
hsa-miR-425-5p	4.917363749	34.9313247	5.994724118
hsa-miR-4259	1.37179534	9.744780104	3.714713499
hsa-miR-4274	1.653315521	11.7446063	4.024114051
hsa-miR-4281	9.817200194	69.73814122	12.26005643
hsa-miR-4284	10.63253305	75.52999597	12.88839682
hsa-miR-4286	10.13008898	71.96079963	12.26005643
hsa-miR-4290	2.298701585	16.32921532	5.032584172
hsa-miR-4291	2.547862817	18.09917425	4.798541198
hsa-miR-4298	5.512091705	39.15607527	8.962374449
hsa-miR-4299	6.196038079	44.01460396	7.047227741
hsa-miR-4306	4.970258284	35.30706997	5.567690079
hsa-miR-4312	1.981447562	14.07554773	4.546875495
hsa-miR-4313	4.137015132	29.38798637	5.354448634
hsa-miR-4327	4.357748635	30.95600413	7.047227741
hsa-miR-449a	2.257026606	16.03317006	4.949522624
hsa-miR-449b-3p	2.841666032	20.18625506	5.164175203
hsa-miR-449c-3p	2.132960588	15.15184612	4.74185466
hsa-miR-450a-5p	1.62227387	11.52409669	4.097587661
hsa-miR-455-3p	4.859824581	34.52258549	6.72659457
hsa-miR-455-5p	2.852716444	20.26475353	5.523791743
hsa-miR-484	3.507815356	24.91835939	4.7701092
hsa-miR-485-3p	1.931620513	13.72159287	4.889324858
hsa-miR-491-3p	2.79097818	19.82618533	5.749949854
hsa-miR-494	8.283241846	58.84140877	9.2666837
hsa-miR-498	2.042204194	14.50714273	4.128734764
hsa-miR-500a-3p	2.531922596	17.98594019	4.393786163
hsa-miR-500a-5p	2.013446043	14.30285435	3.836693986
hsa-miR-502-3p	1.809240846	12.85224821	3.886555557
hsa-miR-502-5p	1.490801471	10.59016028	3.625588668
hsa-miR-505-3p	4.297800682	30.53015371	5.2540446
hsa-miR-505-5p	2.540686049	18.04819286	3.779902166
hsa-miR-513a-5p	3.157323374	22.42858035	5.994724118
hsa-miR-514b-3p	1.382131538	9.818205037	3.828411682
hsa-miR-514b-5p	1.902062062	13.51161941	4.646466678
hsa-miR-520b	2.658295224	18.88364952	6.317471652
hsa-miR-520e	2.203213737	15.65090125	4.660504415
hsa-miR-542-3p	1.510684728	10.73140435	3.537066614
hsa-miR-548c-5p	1.908237818	13.55548994	4.993857538
hsa-miR-548d-5p	1.665941498	11.83429706	5.077772801
hsa-miR-548q	1.884876552	13.38953924	4.033989956
hsa-miR-548y	1.590730845	11.30002548	4.798541198
hsa-miR-572	5.299110117	37.64312455	8.351444508
hsa-miR-574-3p	6.738285613	47.86655099	8.307345268
hsa-miR-574-5p	6.309902776	44.82346109	7.529016836
hsa-miR-575	5.508253983	39.12881336	7.360508577
hsa-miR-576-3p	1.441526988	10.24013065	4.481761629
hsa-miR-583	2.349409727	16.68942917	5.618428218
hsa-miR-584-5p	1.953219225	13.87502296	4.204958561
hsa-miR-590-5p	3.62519098	25.75215698	4.92801709

hsa-miR-595	2.533720676	17.99871316	4.426959826
hsa-miR-601	2.495110907	17.72444214	5.523791743
hsa-miR-622	1.987259396	14.11683307	3.836693986
hsa-miR-623	2.102125464	14.93280361	4.565506063
hsa-miR-629-3p	2.576928339	18.3056461	4.74185466
hsa-miR-636	2.87515986	20.42418413	5.941433092
hsa-miR-638	7.871257032	55.914805	11.26571402
hsa-miR-654-3p	1.577967188	11.20935668	3.919572726
hsa-miR-654-5p	1.988699375	14.12706221	3.828411682
hsa-miR-660-5p	4.883626779	34.69166842	6.457343715
hsa-miR-670	2.181052967	15.49347847	3.652512778
hsa-miR-671-5p	3.572143416	25.37532464	8.389540218
hsa-miR-708-5p	2.188349404	15.54530994	5.052081488
hsa-miR-720	12.96589229	92.10540783	14.07723238
hsa-miR-744-5p	3.261608841	23.16938979	5.643112092
hsa-miR-762	6.884747527	48.90696795	9.023659859
hsa-miR-764	1.417116093	10.06672374	3.662623558
hsa-miR-765	2.803470829	19.91492897	6.256605335
hsa-miR-766-3p	3.844533615	27.31029447	5.889589913
hsa-miR-769-5p	1.776484643	12.61955898	4.024114051
hsa-miR-874	5.604346965	39.8114261	7.529016836
hsa-miR-892b	1.894749864	13.45967598	3.850146141
hsa-miR-937	2.072552938	14.72273017	4.576235395
hsa-miR-939	5.706233587	40.53519495	7.851199509
hsa-miR-940	6.790849694	48.23994883	8.696390017
hsa-miR-96-5p	4.977460703	35.35823356	6.773394597

CYTES

Relative max. intensity (%)	Times detected (%)	Chromosome Band
33.80695194	54.54545455	22q13.31
36.90897916	90.90909091	19q13.41
26.65713942	18.18181818	9q22.32
28.65612962	18.18181818	20q13.33 /// 18q11.2
65.35646358	100	10q23.31
64.50413344	100	6q25.3
73.66380382	100	8q24.21
91.55490564	100	18q21.31
44.87722788	100	3q27.1
37.19433597	100	16p13.3
64.50413344	100	16p13.3
45.69673148	36.36363636	3p21.31
42.96019866	100	12q13.3
39.3081421	36.36363636	12q13.3
46.29696836	100	8q24.3
29.99473375	90.90909091	11q13.1
38.37840372	100	19p13.2
91.55490564	100	2q31.1
26.85117404	36.36363636	22q13.31
25.94624199	9.090909091	2q31.3
39.3081421	81.81818182	19q13.41
58.59795924	100	11q24.1 /// 21q21.1
47.92116392	72.72727273	9q34.3
70.68998485	100	11q21
63.32381836	100	17q25.3
67.79195098	100	6p21.31
41.65163006	100	2q21.3 /// 3p22.3
49.72886077	100	22q13.2
31.1329829	81.81818182	17p11.2
68.80569746	100	1p36.13
27.25460434	45.45454545	10q21.3
46.09447	100	4q34.3
29.7756702	27.27272727	6p12.2
37.88487587	100	3p21.1 /// 12q23.1
37.88487587	81.81818182	16q22.1
36.28862165	36.36363636	2q37.1
66.37535654	100	7p15.2
44.87722788	100	12q13.13
51.0145556	100	19q13.33
38.84355064	90.90909091	8q24.3
56.17816998	100	8q24.3
29.65226106	63.63636364	21q21.3
68.80569746	100	13q14.2 /// 3q25.33
39.81671929	90.90909091	13q31.3
49.72886077	100	1q32.1 /// 9q33.3

35.35885099	90.90909091	1q32.1 /// 9q33.3
46.95273427	100	20q11.21
37.32299404	81.81818182	7q32.2
35.26541808	90.90909091	22q11.21
32.50806176	81.81818182	1p31.1
65.82745424	100	Xp11.23
29.0021455	36.36363636	19p13.3
35.1597707	100	3p21.31
29.87063401	18.18181818	16q24.1
36.37239634	100	20q13.33
75.6858563	100	10p12.31
39.81671929	100	17q11.2
56.03510751	100	1p13.3
48.95370121	100	4q26
37.32299404	36.36363636	3q13.33
34.08724862	72.72727273	14q32.33
33.48248264	36.36363636	1q32.2
31.02080922	72.72727273	13q31.3
91.55490564	100	17q23.1
59.32589791	90.90909091	11p15.5
26.77206232	9.090909091	15q13.3
55.5111026	90.90909091	4p15.31 /// 5q34
29.52354874	63.63636364	17p13.3
42.96019866	100	Xp11.3
41.65163006	100	Xq28
39.55102772	54.54545455	13q12.12
65.82745424	100	19p13.13
65.35646358	100	9q22.32
65.11894677	100	9q22.32 /// 19p13.13
57.96265499	100	7q22.1
62.3852184	100	3p22.2 /// 12q14.1
65.35646358	100	2q35
58.59795924	100	19p13.13
66.37535654	100	9q22.32
42.76518346	90.90909091	3q28
83.65920458	100	9q34.11
32.21274654	63.63636364	6q13
52.98148807	100	6q13
56.41050324	100	8q24.22
40.6103749	90.90909091	1p34.2 /// 6q13
31.8369514	72.72727273	1p34.2
48.95370121	100	1p34.2
27.01795066	45.45454545	9p21.3
37.19433597	45.45454545	9p21.3
28.49473079	27.27272727	1q44
36.1633607	100	2p24.3
41.44416096	72.72727273	2q11.2
29.10790666	36.36363636	3q29
31.2120028	36.36363636	4p16.1

60.34269268	100	5q33.2
29.99473375	54.54545455	8p12
35.26541808	54.54545455	10q11.21 /// 18p11.21 /// 21q11.2
66.97582058	100	11q12.1
25.5427979	27.27272727	19p13.11
28.49473079	36.36363636	19q13.32
28.17442596	36.36363636	20q13.2
61.29955244	100	20q13.33
62.0859822	100	20q13.33
45.87083272	100	22q11.21 /// 12q13.13
27.09483559	45.45454545	9q31.3
57.10976563	100	8p21.3
65.35646358	100	1p13.1 /// 1q42.11
70.68998485	100	18q11.2 /// 18q11.2
66.97582058	100	13q14.11 /// Xq27.1
65.11894677	100	19q13.32
46.09447	100	17p13.1
38.84355064	90.90909091	17p13.1
60.34269268	100	12q22
27.50638306	54.54545455	17q25.3
26.65713942	45.45454545	22q13.2
39.98393738	90.90909091	5q35.3
48.95370121	100	14q32.2
37.70412365	54.54545455	14q32.2
35.35885099	90.90909091	15q26.1
44.280255	45.45454545	8q24.11
31.8369514	27.27272727	13q14.2
37.88487587	90.90909091	Xp11.23
37.55906726	72.72727273	Xp11.23
30.32275189	36.36363636	1q42.13
38.98217989	36.36363636	20q13.12
66.37535654	100	9q22.31
45.87083272	81.81818182	22q12.2
72.50996603	100	11q23.3
60.0249981	100	17q11.2
91.55490564	100	13q22.3
56.86269397	36.36363636	22q13.33
32.69609225	100	17p13.1
66.97582058	100	2q21.2
31.2120028	27.27272727	6q25.3
26.85117404	36.36363636	15q24.3
59.0126315	100	Xq13.2
30.64575844	63.63636364	2q35
25.30400138	36.36363636	1p36.11
35.26541808	36.36363636	16q12.2
29.19258242	36.36363636	Xp11.4
27.09483559	18.18181818	19p13.3
30.64575844	36.36363636	15q22.31
25.94624199	54.54545455	17q11.2
48.37702283	100	17q11.2

36.54077564	100	3p21.31
42.58453621	100	3p21.31
26.38809533	9.090909091	1q23.2
28.58597446	27.27272727	4p16.1
87.09138348	100	5q35.2
91.55490564	100	7q11.23
87.09138348	100	8p23.1
35.74981245	54.54545455	9q22.2
34.08724862	45.45454545	9q22.32
63.66574202	100	11p15.5
50.06117362	100	11p15.3
39.55102772	100	13q32.3
32.29949875	36.36363636	15q23
38.03623107	100	15q24.2
50.06117362	90.90909091	21q22.11
35.1597707	45.45454545	5q11.2
36.68459158	72.72727273	5q11.2
33.68456621	45.45454545	5q11.2
29.10790666	18.18181818	Xq26.3 /// Xq26.3
47.78350169	90.90909091	9q32
39.23918846	45.45454545	9q32
33.88527711	90.90909091	16p13.11
34.73214569	36.36363636	14q32.31
40.84574084	72.72727273	9p21.3
65.82745424	100	14q32.31
29.32916537	36.36363636	19q13.42
31.2120028	63.63636364	Xp11.23
27.25460434	54.54545455	Xp11.23
27.60880444	36.36363636	Xp11.23
25.75498202	18.18181818	Xp11.23
37.32299404	100	Xq27.1
26.85117404	72.72727273	Xq27.1
42.58453621	81.81818182	Xq27.3 /// Xq27.3
27.1957696	9.090909091	Xq27.3
33.00696156	36.36363636	Xq27.3
44.87722788	36.36363636	19q13.42
33.10668099	36.36363636	19q13.42
25.12615065	18.18181818	Xq26.3
35.47471125	45.45454545	12q14.2
36.07081751	18.18181818	8q24.13 /// 17q24.2
28.65612962	36.36363636	10p13
34.08724862	18.18181818	14q21.3
59.32589791	100	4p15.33
59.0126315	100	4p14
53.48364391	100	4p14
52.286617	100	4q21.22
31.8369514	9.090909091	4q25
39.91145467	36.36363636	5q15
29.87063401	36.36363636	5q32
35.0070025	90.90909091	7q11.23

31.44765752	54.54545455	7q36.3
39.23918846	36.36363636	9q33.3
27.25460434	36.36363636	13q31.3
32.43184414	36.36363636	13q32.3
33.68456621	54.54545455	15q23
42.20597439	54.54545455	17q25.1
80.02790407	100	19p13.2
27.84334748	27.27272727	14q32.31
27.1957696	36.36363636	14q32.31
45.87083272	100	Xp11.23
25.94624199	54.54545455	11p11.2
59.59651722	45.45454545	7q36.1
35.88831493	36.36363636	11q14.1
100	100	3q26.1
40.08680074	63.63636364	17p12
64.1010933	100	16p11.2
26.01806562	18.18181818	Xq23
44.4448537	54.54545455	1q23.1
41.83769761	90.90909091	Xq24
28.58597446	27.27272727	19q13.32
53.48364391	100	5q31.2
27.350164	36.36363636	Xq27.3
32.50806176	54.54545455	8q24.3
55.77232299	100	8q24.3
61.77627664	100	16p13.3
48.11595359	90.90909091	7q32.2

Description
ACC=MI0000063; ID=hsa-let-7b
ACC=MI0000066; ID=hsa-let-7e
ACC=MI0000067; ID=hsa-let-7f-1
ACC=MI0000651; ID=hsa-mir-1-1 /// ACC=MI0000437; ID=hsa-mir-1-2
ACC=MI0000114; ID=hsa-mir-107
ACC=MI0006334; ID=hsa-mir-1202
ACC=MI0006340; ID=hsa-mir-1207
ACC=MI0000442; ID=hsa-mir-122
ACC=MI0003764; ID=hsa-mir-1224
ACC=MI0006311; ID=hsa-mir-1225
ACC=MI0006311; ID=hsa-mir-1225
ACC=MI0006313; ID=hsa-mir-1226
ACC=MI0006318; ID=hsa-mir-1228
ACC=MI0006318; ID=hsa-mir-1228
ACC=MI0006324; ID=hsa-mir-1234
ACC=MI0006327; ID=hsa-mir-1237
ACC=MI0006328; ID=hsa-mir-1238
ACC=MI0006381; ID=hsa-mir-1246
ACC=MI0006384; ID=hsa-mir-1249
ACC=MI0006392; ID=hsa-mir-1258
ACC=MI0000469; ID=hsa-mir-125a
ACC=MI0000446; ID=hsa-mir-125b-1 /// ACC=MI0000470; ID=hsa-mir-125b-2
ACC=MI0000471; ID=hsa-mir-126
ACC=MI0014197; ID=hsa-mir-1260b
ACC=MI0016748; ID=hsa-mir-1268b
ACC=MI0006415; ID=hsa-mir-1275
ACC=MI0000447; ID=hsa-mir-128-1 /// ACC=MI0000727; ID=hsa-mir-128-2
ACC=MI0006428; ID=hsa-mir-1281
ACC=MI0006432; ID=hsa-mir-1288
ACC=MI0006352; ID=hsa-mir-1290
ACC=MI0003780; ID=hsa-mir-1296
ACC=MI0006372; ID=hsa-mir-1305
ACC=MI0000822; ID=hsa-mir-133b
ACC=MI0000452; ID=hsa-mir-135a-1 /// ACC=MI0000453; ID=hsa-mir-135a-2
ACC=MI0000456; ID=hsa-mir-140
ACC=MI0007076; ID=hsa-mir-1471
ACC=MI0000253; ID=hsa-mir-148a
ACC=MI0000811; ID=hsa-mir-148b
ACC=MI0000479; ID=hsa-mir-150
ACC=MI0000809; ID=hsa-mir-151a
ACC=MI0000809; ID=hsa-mir-151a
ACC=MI0000681; ID=hsa-mir-155
ACC=MI0000070; ID=hsa-mir-16-1 /// ACC=MI0000115; ID=hsa-mir-16-2
ACC=MI0000071; ID=hsa-mir-17
ACC=MI0000289; ID=hsa-mir-181a-1 /// ACC=MI0000269; ID=hsa-mir-181a-2

ACC=MI0000270; ID=hsa-mir-181b-1 /// ACC=MI0000683; ID=hsa-mir-181b-2
ACC=MI0008193; ID=hsa-mir-1825
ACC=MI0000273; ID=hsa-mir-183
ACC=MI0000482; ID=hsa-mir-185
ACC=MI0000483; ID=hsa-mir-186
ACC=MI0000484; ID=hsa-mir-188
ACC=MI0008330; ID=hsa-mir-1909
ACC=MI0000465; ID=hsa-mir-191
ACC=MI0008331; ID=hsa-mir-1910
ACC=MI0008335; ID=hsa-mir-1914
ACC=MI0008336; ID=hsa-mir-1915
ACC=MI0000487; ID=hsa-mir-193a
ACC=MI0000239; ID=hsa-mir-197
ACC=MI0009983; ID=hsa-mir-1973
ACC=MI0000240; ID=hsa-mir-198
ACC=MI0000283; ID=hsa-mir-203
ACC=MI0000285; ID=hsa-mir-205
ACC=MI0000076; ID=hsa-mir-20a
ACC=MI0000077; ID=hsa-mir-21
ACC=MI0000286; ID=hsa-mir-210
ACC=MI0000287; ID=hsa-mir-211
ACC=MI0000294; ID=hsa-mir-218-1 /// ACC=MI0000295; ID=hsa-mir-218-2
ACC=MI0000078; ID=hsa-mir-22
ACC=MI0000298; ID=hsa-mir-221
ACC=MI0000301; ID=hsa-mir-224
ACC=MI0011282; ID=hsa-mir-2276
ACC=MI0000079; ID=hsa-mir-23a
ACC=MI0000439; ID=hsa-mir-23b
ACC=MI0000080; ID=hsa-mir-24-1 /// ACC=MI0000081; ID=hsa-mir-24-2

ACC=MI0000082; ID=hsa-mir-25
ACC=MI0000083; ID=hsa-mir-26a-1 /// ACC=MI0000750; ID=hsa-mir-26a-2
ACC=MI0000084; ID=hsa-mir-26b
ACC=MI0000085; ID=hsa-mir-27a
ACC=MI0000440; ID=hsa-mir-27b
ACC=MI0000086; ID=hsa-mir-28
ACC=MI0013006; ID=hsa-mir-2861
ACC=MI0000088; ID=hsa-mir-30a
ACC=MI0000088; ID=hsa-mir-30a
ACC=MI0000441; ID=hsa-mir-30b
ACC=MI0000736; ID=hsa-mir-30c-1 /// ACC=MI0000254; ID=hsa-mir-30c-2
ACC=MI0000749; ID=hsa-mir-30e
ACC=MI0000749; ID=hsa-mir-30e
ACC=MI0000089; ID=hsa-mir-31
ACC=MI0000089; ID=hsa-mir-31
ACC=MI0014140; ID=hsa-mir-3124
ACC=MI0014142; ID=hsa-mir-3125
ACC=MI0014144; ID=hsa-mir-3127
ACC=MI0014160; ID=hsa-mir-3137
ACC=MI0014161; ID=hsa-mir-3138

ACC=MI0014165; ID=hsa-mir-3141
ACC=MI0014175; ID=hsa-mir-3148
ACC=MI0014184; ID=hsa-mir-3156-1 /// ACC=MI0014230; ID=hsa-mir-3156-2 /// ACC=MI0014242; ID=hsa
ACC=MI0014192; ID=hsa-mir-3162
ACC=MI0014233; ID=hsa-mir-3189
ACC=MI0014236; ID=hsa-mir-3191
ACC=MI0014239; ID=hsa-mir-3194
ACC=MI0014240; ID=hsa-mir-3195
ACC=MI0014241; ID=hsa-mir-3196
ACC=MI0014246; ID=hsa-mir-3198-1 /// ACC=MI0017335; ID=hsa-mir-3198-2
ACC=MI0000090; ID=hsa-mir-32
ACC=MI0000542; ID=hsa-mir-320a
ACC=MI0003776; ID=hsa-mir-320b-1 /// ACC=MI0003839; ID=hsa-mir-320b-2
ACC=MI0003778; ID=hsa-mir-320c-1 /// ACC=MI0008191; ID=hsa-mir-320c-2
ACC=MI0008190; ID=hsa-mir-320d-1 /// ACC=MI0008192; ID=hsa-mir-320d-2
ACC=MI0014234; ID=hsa-mir-320e
ACC=MI0000813; ID=hsa-mir-324
ACC=MI0000813; ID=hsa-mir-324
ACC=MI0000812; ID=hsa-mir-331
ACC=MI0000814; ID=hsa-mir-338
ACC=MI0000091; ID=hsa-mir-33a
ACC=MI0000802; ID=hsa-mir-340
ACC=MI0000805; ID=hsa-mir-342
ACC=MI0000825; ID=hsa-mir-345
ACC=MI0017351; ID=hsa-mir-3529
ACC=MI0016000; ID=hsa-mir-3610
ACC=MI0016003; ID=hsa-mir-3613
ACC=MI0000762; ID=hsa-mir-362
ACC=MI0000762; ID=hsa-mir-362
ACC=MI0016011; ID=hsa-mir-3620
ACC=MI0016046; ID=hsa-mir-3646
ACC=MI0016051; ID=hsa-mir-3651
ACC=MI0016053; ID=hsa-mir-3653
ACC=MI0016056; ID=hsa-mir-3656
ACC=MI0000769; ID=hsa-mir-365b
ACC=MI0016066; ID=hsa-mir-3665
ACC=MI0016068; ID=hsa-mir-3667
ACC=MI0016077; ID=hsa-mir-3676
ACC=MI0016080; ID=hsa-mir-3679
ACC=MI0016093; ID=hsa-mir-3692
ACC=MI0016134; ID=hsa-mir-3713
ACC=MI0000782; ID=hsa-mir-374a
ACC=MI0000783; ID=hsa-mir-375
ACC=MI0016423; ID=hsa-mir-3917
ACC=MI0016591; ID=hsa-mir-3935
ACC=MI0016593; ID=hsa-mir-3937
ACC=MI0016597; ID=hsa-mir-3940
ACC=MI0001444; ID=hsa-mir-422a
ACC=MI0001445; ID=hsa-mir-423
ACC=MI0001445; ID=hsa-mir-423

ACC=MI0001448; ID=hsa-mir-425
ACC=MI0001448; ID=hsa-mir-425
ACC=MI0015858; ID=hsa-mir-4259
ACC=MI0015884; ID=hsa-mir-4274
ACC=MI0015885; ID=hsa-mir-4281
ACC=MI0015893; ID=hsa-mir-4284
ACC=MI0015894; ID=hsa-mir-4286
ACC=MI0015899; ID=hsa-mir-4290
ACC=MI0015900; ID=hsa-mir-4291
ACC=MI0015830; ID=hsa-mir-4298
ACC=MI0015829; ID=hsa-mir-4299
ACC=MI0015836; ID=hsa-mir-4306
ACC=MI0015842; ID=hsa-mir-4312
ACC=MI0015843; ID=hsa-mir-4313
ACC=MI0015867; ID=hsa-mir-4327
ACC=MI0001648; ID=hsa-mir-449a
ACC=MI0003673; ID=hsa-mir-449b
ACC=MI0003823; ID=hsa-mir-449c
ACC=MI0001652; ID=hsa-mir-450a-1 /// ACC=MI0003187; ID=hsa-mir-450a-2
ACC=MI0003513; ID=hsa-mir-455
ACC=MI0003513; ID=hsa-mir-455
ACC=MI0002468; ID=hsa-mir-484
ACC=MI0002469; ID=hsa-mir-485
ACC=MI0003126; ID=hsa-mir-491
ACC=MI0003134; ID=hsa-mir-494
ACC=MI0003142; ID=hsa-mir-498
ACC=MI0003184; ID=hsa-mir-500a
ACC=MI0003184; ID=hsa-mir-500a
ACC=MI0003186; ID=hsa-mir-502
ACC=MI0003186; ID=hsa-mir-502
ACC=MI0003190; ID=hsa-mir-505
ACC=MI0003190; ID=hsa-mir-505
ACC=MI0003191; ID=hsa-mir-513a-1 /// ACC=MI0003192; ID=hsa-mir-513a-2
ACC=MI0014251; ID=hsa-mir-514b
ACC=MI0014251; ID=hsa-mir-514b
ACC=MI0003155; ID=hsa-mir-520b
ACC=MI0003143; ID=hsa-mir-520e
ACC=MI0003686; ID=hsa-mir-542
ACC=MI0003630; ID=hsa-mir-548c
ACC=MI0003668; ID=hsa-mir-548d-1 /// ACC=MI0003671; ID=hsa-mir-548d-2
ACC=MI0010637; ID=hsa-mir-548q
ACC=MI0016595; ID=hsa-mir-548y
ACC=MI0003579; ID=hsa-mir-572
ACC=MI0003581; ID=hsa-mir-574
ACC=MI0003581; ID=hsa-mir-574
ACC=MI0003582; ID=hsa-mir-575
ACC=MI0003583; ID=hsa-mir-576
ACC=MI0003590; ID=hsa-mir-583
ACC=MI0003591; ID=hsa-mir-584
ACC=MI0003602; ID=hsa-mir-590

ACC=MI0003607; ID=hsa-mir-595
ACC=MI0003614; ID=hsa-mir-601
ACC=MI0003636; ID=hsa-mir-622
ACC=MI0003637; ID=hsa-mir-623
ACC=MI0003643; ID=hsa-mir-629
ACC=MI0003651; ID=hsa-mir-636
ACC=MI0003653; ID=hsa-mir-638
ACC=MI0003676; ID=hsa-mir-654
ACC=MI0003676; ID=hsa-mir-654
ACC=MI0003684; ID=hsa-mir-660
ACC=MI0003933; ID=hsa-mir-670
ACC=MI0003760; ID=hsa-mir-671
ACC=MI0005543; ID=hsa-mir-708
ACC=MI0006654; ID=hsa-mir-720
ACC=MI0005559; ID=hsa-mir-744
ACC=MI0003892; ID=hsa-mir-762
ACC=MI0003944; ID=hsa-mir-764
ACC=MI0005116; ID=hsa-mir-765
ACC=MI0003836; ID=hsa-mir-766
ACC=MI0003834; ID=hsa-mir-769
ACC=MI0005532; ID=hsa-mir-874
ACC=MI0005538; ID=hsa-mir-892b
ACC=MI0005759; ID=hsa-mir-937
ACC=MI0005761; ID=hsa-mir-939
ACC=MI0005762; ID=hsa-mir-940
ACC=MI0000098; ID=hsa-mir-96

-mir-3156-3

Supplementary Table 3

A)

mRNA/microRNA	Predicted consequential pairing of target region (top) and microRNA (bottom)
Position 639-645 of SULT2A1 3' UTR hsa-miR-324-5p	5' ...AGGGUUCAAAGCCCA--GGGAUGCA... 3' UGUGGUUACGGGAUCCCCUACGC

mRNA/microRNA	Predicted consequential pairing of target region (top) and microRNA (bottom)
Position 266-272 of GSTT1 3' UTR hsa-miR-24	5' ...AAACCUGGGCUCAGCCUGAGCCU... 3' GACAAGGACGACUU---GACUCGGU

B)

Gene/ microRNA	Seed Match	Context + score percentile
SULT2A1/ hsa-miR- 324-5p	8mer	96
GSTT1/ has-miR-24-3p	7mer-m8	84

C)

microRNA/ Gene (symbol)	Accession Number (miRBase)	
hsa-miR-324-5p	MI0000813 / MIMAT0000761	
hsa-miR-24-3p	MI0000080 / MIMAT0000080	
	UniGene	GeneBank
SULT2A1	Hs.515835	NM_003167
GSTT1	Hs.268573	NM_000853

Supplementary Table 4

Name	Host	Dilution	Source
Primary Antibody			
SULT2A1	Rabbit polyclonal	1:250	Abcam
GSTT1	Rabbit polyclonal	1:500	Abcam
ABCG2	Mouse monoclonal	1:100	Abcam
ABCC1	Mouse monoclonal	1:50	Abcam
Secondary Antibody			
Alexa Fluor 568	Goat	1:400	Invitrogen
Alexa Fluor 488	Rabbit	1:400	Invitrogen
Name	**Ref Number**		**Source**
Genes			
SULT2A1	Hs00234219_m1 (Taqman)		Applied Biosystems
GSTT1	Hs00184475_m1 (Taqman)		Applied Biosystems

Supplementary Table 5

A)

STUDY NO.	AGE	OUTCOME	ALT (IU/L)	CREATININE (umol/L)	BILIRUBIN (umol/L)	INR RATIO (ratio)
1	29	Died	8696	241	64	11.5
8	38	Survived	5699	272	77	8.7
58	33	Survived	9424	216	48	3

B)

THE NORMAL RANGES	
NAME	**RANGE (UNIT)**
ALT	10-50 (IU/L)
CREATININE	30-120 (umol/L)
BILIRUBIN	3-17 (umol/L)
INR	0.8-1.2 (RATIO)

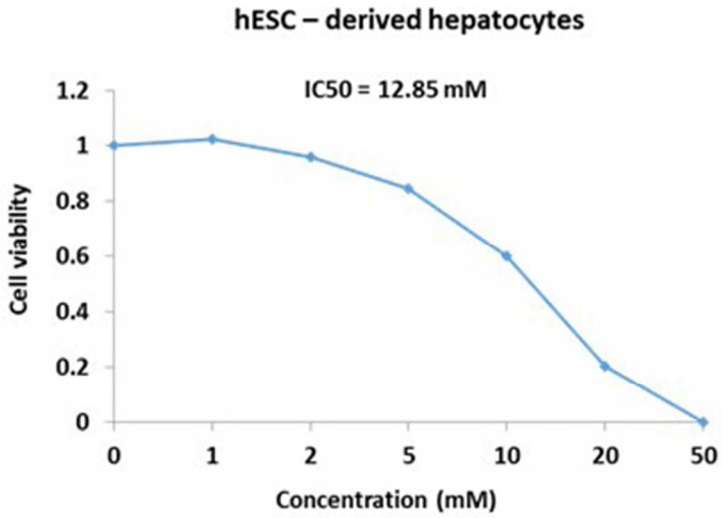

Graphical abstract
96x73mm (96 x 96 DPI)